AEDC-TR-65-260

IONIZATION AND RECOMBINATION IN ALKALI-SEEDED COLLISION-DOMINATED PLASMAS

B. P. Curry
ARO, Inc.

February 1966

PROPULSION WIND TUNNEL FACILITY
ARNOLD ENGINEERING DEVELOPMENT CENTER
AIR FORCE SYSTEMS COMMAND
ARNOLD AIR FORCE STATION, TENNESSEE

NOTICES

When U. S. Government drawings specifications, or other data are used for any purpose other than a definitely related Government procurement operation, the Government thereby incurs no responsibility nor any obligation whatsoever, and the fact that the Government may have formulated, furnished, or in any way supplied the said drawings, specifications, or other data, is not to be regarded by implication or otherwise, or in any manner licensing the holder or any other person or corporation, or conveying any rights or permission to manufacture, use, or sell any patented invention that may in any way be related thereto.

Qualified users may obtain copies of this report from the Defense Documentation Center.

References to named commercial products in this report are not to be considered in any sense as an endorsement of the product by the United States Air Force or the Government.

IONIZATION AND RECOMBINATION IN ALKALI-SEEDED COLLISION-DOMINATED PLASMAS

B. P. Curry
ARO, Inc.

AF - AEDC
Arnold AFS Tenn

FOREWORD

The research reported herein was submitted by the author as a thesis to the graduate council of the University of Tennessee in partial fulfillment of the requirements for the degree of Master of Science. The investigation was performed at the Propulsion Wind Tunnel Facility (PWT) of the Arnold Engineering Development Center (AEDC), Air Force Systems Command (AFSC) by personnel of ARO, Inc. (a subsidiary of Sverdrup and Parcel, Inc.), contract operator of the AEDC, under Contract AF 40(600)-1200. The Program Element Number was 65402234, and the ARO Project No. was PT8002. The manuscript was submitted for publication on October 12, 1965.

The author acknowledges his indebtedness to Dr. L. E. Ring, Manager, PWT Research Branch, and Dr. J. B. Dicks, Prof. Physics at the University of Tennessee Space Institute, for guidance during the course of this work. The author's colleagues, M. D. High, W. E. Powers, and P. W. Johnson, are also acknowledged for many helpful discussions.

This technical report has been reviewed and is approved.

R. H. LaBounty
1st Lieutenant, USAF
Experimental Branch
DCS/Plans and Technology

Donald D. Carlson
Colonel, USAF
DCS/Plans and Technology

ABSTRACT

At electron densities greater than 10^{12}/cc, ionization and recombination proceed predominantly by sequential transitions between adjacent energy levels induced by collisions with free electrons. Similar models for this process have been developed by various investigators. This report develops closed-form expressions for ionization and recombination of effective one-electron atoms by modifying the Byron model and determining analytically the critical energy level in equilibrium with the free electrons, using a simplified quantum mechanical model of the alkali atoms. The reaction rate coefficients calculated from these expressions agree satisfactorily with available experimental data and with numerical calculations of other investigators.

CONTENTS

ILLUSTRATIONS

TABLES

NOMENCLATURE

$A_{c,\,c-1}$	Einstein's probability coefficient for radiative transitions across the critical interval
a_1	First Bohr radius of hydrogen
B	Dimensionless slope in Byron's linearization of Gryzinski's cross section appearing in Eq. (33)
E	Difference between initial and final atomic energy levels in a collision-induced transition
E_1	Initial atomic energy level before a collision-induced transition
$F\left(\frac{\Delta\epsilon}{kT_e}\right)$	Collision integral defined by Eq. (24)
f	Oscillator strength appearing in Eq. (38)
$f(\vec{v}_e)$	Maxwell-Boltzmann electron velocity distribution
$\mathfrak{Z}$	Reaction rate ratio defined by Eq. (9)
g_i	Degeneracy of the "ith" state
g_j	Dimensionless Gryzinski cross-section function defined by Eq. (31)
$\bar{g}$	Average degeneracy of the substates within the critical interval
h	Planck's constant
j	Parameter defined by Eq. (13)
K	Reaction rate coefficients (see Eqs. (36) and (37))
k	Boltzmann's constant
ℓ	Orbital angular momentum quantum number
ℓ'	Effective angular momentum quantum number defined by Eq. (12)

m_e	Electron mass
N	Principal quantum number
N'	Effective principal quantum number defined by Eq. (17)
n_e	Free-electron number density
n_i	Number density of the "ith" state
$Q_{(E)}$	Cross section for collision-induced transition across interval E
$\overline{Q}$	Cross section averaged over a Maxwell-Boltzmann distribution of electron velocities
q_e	Electronic charge
R	Radial wave function for valence electron
r	Radial coordinate of valence electron
S,P,D,F	Atomic spectral state notation
T_e	Free-electron temperature
$V_{(r)}$	Potential energy function for valence electron
v_e	Electron speed
$\bar{v}_e$	Average thermal electron speed
X	Parameter appearing in Eq. (26)
x	Transformed wave function appearing in Eq. (14)
y	Parameter appearing in Eq. (26)
α	Atomic structure parameter appearing in Eq. (21)
β	Coefficient of non-coulombic portion of $V_{(r)}$
γ	Transformed wave number eigenvalue appearing in Eq. (11)
$\Delta\epsilon$	Critical interval defined by critical energy level and energy level one principal quantum number below the critical level
ϵ	Ionization potential
ϵ_c	Critical state energy level
ϵ_i	"ith" energy level measured from ground state
ϵ_o	Permittivity of free space
κ	Parameter defined by Eq. (13)
μ_e	Reduced electron mass appearing in Eq. (11)

$\nu_{c,c-1}$	Emission frequency for radiative transitions across critical interval
σ_{c1}	Cross section appearing in Thomson-Bohr theory (see Eqs. (7) and (8))
ξ^2	Dimensionless free-electron temperature appearing in Eq. (26)
ζ^2	Dimensionless critical state binding energy appearing in Eq. (26)
χ	Radiative-collisional transition ratio (see Eq. (40))

SUBSCRIPTS

0	Ground state
1	State one principal quantum number above ground state
c	Critical state
c-1	State one principal quantum number below critical state

SECTION I
INTRODUCTION

For many years physicists have been concerned with the mechanisms of ionization and recombination in both laboratory and stellar plasmas. Recently new impetus has been given to these studies by two potential applications of plasma physics: the thermonuclear program and the development of magnetohydrodynamic (MHD) energy conversion techniques. In the latter case research has concentrated on achieving conductivities sufficient for practical devices by seeding plasmas with small amounts of alkali metals. As a result electron densities of 10^{14} - 10^{15}/cc can be attained at plasma temperatures low enough that conventional gas dynamic channels can be used for containment of the plasma. Because the gas velocity in such channels is usually quite high (on the order of 1000 m/sec), there are conditions under which a sizable fraction of the channel length is required for a perturbed plasma to reach equilibrium conditions. Even when equilibrium conditions prevail in the center of the channel, one normally finds that equilibrium conditions are not maintained near the electrodes. Under these conditions it is necessary to know the ionization and recombination rates in alkali-seeded plasmas to fully understand the flow.

There are various mechanisms of recombination in plasmas: dissociative recombination of molecular ions, radiative recombination, dielectronic recombination, three-body recombination with a neutral particle participating as the third body to conserve momentum, and three-body recombination with an electron acting as the third body. The associated mechanisms of ionization are listed respectively: associative atom-atom collision-induced ionization, photoionization, autoionization, atom-atom or atom-molecule collision-induced ionization, and electron-atom or electron-molecule collision-induced ionization.

Although different mechanisms prevail in atmospheric plasmas, conditions occurring in laboratory plasmas and practical MHD devices are dominated by collision-induced ionization and recombination with proper account taken of radiative effects.

Understanding of the general process has come about only recently. Massey and Burhop (Ref. 1) indicate that, at the time of their publication, recombination in high density afterglows resembled, but exceeded by several orders of magnitude, pure radiative recombination. In an effort to explain the anamolously large electron loss occurring in the B-1 Stellerator, D'Angelo (Ref. 2) applied the theories of non-thermal equilibrium in stellar atmospheres developed in Refs. 3 and 4 to the calculation

of three-body (electron-electron-ion) recombination into excited states of the resulting neutral atoms. He assumed that these excited states decayed further only by radiant emission. Using the available transition probabilities, D'Angelo computed the total rate of recombination into the ground state from all possible combinations of three-body recombination into an excited state followed by radiative cascading downward from that state. His results were much larger than those caused by radiative recombination alone; however, he underestimated the results of experiments reported in Refs. 5 and 6 by about an order of magnitude and, more importantly, obtained an incorrect dependence on electron temperature and density.

During this time Bates, Kingston, and McWhirter in several publications developed a statistical model of the process, culminating in their two authoritative papers on collisional-radiative recombination (Refs. 7 and 8). This model, which gave better agreement with experiments than D'Angelo's, considers the interaction of radiative recombination, three-body recombination into excited states, radiative and collisional cascading between states, and excitation and ionization from various states. Precise quantum mechanical expressions were used for the various radiative transistions, and the semiclassical cross sections of Gryzinski (Ref. 9) were used for the collisional transitions. Qualitative information on the behavior of alkali plasmas was obtained by making the first excited state of hydrogen the ground state of a fictitious substance having a potential well about the depth of that of cesium. The results indicated a similarity of behavior of hydrogen and alkali plasmas.

At about the same time, Hinnov and Hirschberg (Ref. 10) developed a theory to correlate the Stellerator experiments by determining separately collisional and radiative recombination coefficients. In their paper collisional transition rates between all states up to some state in equilibrium with the free electrons were determined by using Thomson-Bohr cross sections. The lowermost state in equilibrium with free electrons, denoted henceforth as the critical-state, was located by assuming detailed balance for excitation and de-excitation of this state by collisions and radiative transitions. The resulting relation was evaluated in the limit of high critical quantum number. For electron energies of 0.25 ev or less, the approximate collisional recombination coefficient obtained by this method for hydrogen is $5.6 \times 10^{-27} \left(\frac{k T_e}{q_e}\right)^{-9/2} n_e$ cc/sec. Good agreement with experiments in both hydrogen and helium plasmas was claimed when the radiative recombination coefficient was added to the results quoted above.

Byron, et al. (Ref. 11) obtained almost identically the same results for hydrogen at high temperature as those of Bates, et al. with the use of the essential simplifications that the transitions of greatest importance are those across the critical state and that the critical state can be located by minimizing the recombination rate with respect to the critical quantum number. Because excited-state population decreases with increasing quantum number, three-body recombination into an excited state increases with increasing quantum number, collisional de-excitation of a given state increases with increasing quantum number, and radiative recombination into a given state decreases with increasing quantum number; they were able to show that the critical quantum number is nearly equal to the larger of the quantum numbers corresponding to the following states: (1) the state at which the collisional de-excitation rate is a minimum and (2) the state at which collisional and radiative de-excitation rates are equal.

Byron, Bortz, and Russel (Ref. 12) applied the same philosophy to computation of collisional recombination rates for potassium, comparing the results with those obtained for hydrogen and argon (the latter having been computed in Ref. 13 from the von Engle ionization theory with the first excitation potential used instead of the ionization potential). Since the critical state could not be determined analytically, the following procedure was used: at a given electron temperature and an assumed critical energy level, the energy levels and degeneracies for all levels between the assumed critical level and the level one principal quantum number below it were obtained from the spectral tables of Ref. 14. The transition rate across this critical interval was then computed at the given electron temperature. The minimum of the curve of transition rates obtained by this procedure then corresponds to the true critical energy level. This tedious calculation must be repeated for each separate electron temperature.

The author (Ref. 15) improved this procedure in the case of alkali metals by finding an analytic approximation for the degeneracy averaged over the substates within the critical interval, making possible an analytic determination of the critical energy level. The results indicated that the behavior (with respect to electron temperature) of the critical energy level can be determined to sufficient accuracy with knowledge required of only the ionization potential, effective ground state quantum number, and the maximum value of the angular momentum quantum number in the interval between the ground state and the state one principal quantum number above ground. This procedure ultimately yields ionization and recombination rates for any element whose quantum mechanical description can be collapsed to that of a one-electron atom (whose potential deviates from coulombic form only in the first order).

Section II of this report presents the formal derivation of the reaction rates in terms of parameters determined in Sections III and IV.

Section III is concerned with how the average degeneracy of states within the critical interval (the interval between the critical energy level and the level one principal quantum number below it) is related to the critical quantum number. The quantum mechanics of a one-electron atom with a potential having an inverse r^2 noncoulombic term is formally presented as suggested in Fermi's notes (Ref. 16). The form of the quantum defect derived by this procedure permits the degeneracy to be averaged over the substates within the critical interval and the result to be related to the critical quantum number and the previously mentioned known quantities. In Section IV the results of Section III are used in the determination of the critical state: the transition equations are minimized with respect to the critical quantum number, making use of the degeneracy relation derived in Section III. All these parameters are ultimately used to obtain the collisional ionization and recombination rates in Section V by means of the equations derived in Section II, and the results are added to available radiative transition information in Section VI to provide a fairly complete treatment of ionization and recombination in moderately dense (10^{12} - 10^{15} electrons/cc) alkali plasmas.

After completion of the research reported herein, the author became aware of a calculation of cesium recombination rates by Dugan (Ref. 17). The Byron procedure was used together with the first 70 energy levels of cesium and results obtained by use of an electronic computer for electron temperatures ranging to 10,000°K. In the temperature range appropriate to the physical restrictions imposed by the present author's approximation technique (0 - 4000°K), Dugan's calculations agree very closely with those of the present theory.

In addition to the experiments of Refs. 5 and 18, which have demonstrated the validity of the general model of collisional radiative recombination for hydrogen and helium afterglows and low density plasma jets, there exists a limited amount of experimental data on cesium recombination (Refs. 19 and 20). In both these references the results, corrected for ambipolar diffusion and other empirical complications, were favorably compared with the theory of Ref. 10 for hydrogen. The present theoretical results for cesium and those of Dugan lie quite close to the aforementioned calculation (and, hence, the experimental data); whereas, the present results for hydrogen are much less. From these and other considerations it is ultimately concluded that the present theory - while not treating collisional - radiative interaction in hydrogen adequately - is reliable within 50 percent (well within the resolution of current experiments) for conditions typical of moderately dense alkali plasmas.

SECTION II
THE GENERAL MODEL

In this section some properties of the general model for collision-dominated ionization and recombination are developed from an empirical point of view and incorporated into the mathematics describing the process. Except for some divergence of point of view in the detailed characteristics of various theories, the derivation presented is more or less common to all considerations of this problem.

The afterglow experiments of Refs. 5 and 6 and the spectrographic studies of low density arc jets of Ref. 18 have demonstrated the following characteristics for hydrogen and helium plasmas: above some critical state all the remaining states obey Boltzmann's distribution law -- i.e., excited-state densities (from spectral intensities) are simple exponentials of principal quantum number. When these population densities are plotted on a semilogarithmic graph against quantum number, the resulting slopes determine the temperature of the excited-state distribution; the result agrees with free electron temperatures determined from conductivity measurements. As recombination progresses, these states remain in transient thermal equilibrium with a time-varying electron temperature. In Refs. 10 and 11 evidence is presented that the deceptive time behavior of the electron concentration, which had for so long prevented identification of three-body decay processes, can be accounted for by the time variation of the recombination rate resulting from the declining electron temperature. The net result of this dual relaxation is an appearance as two-body recombination.

Because the various experiments cited previously have shown that the experimental excited-state densities (for states above some critical level) taken together with the experimental electron temperatures, when substituted into the Saha equation, predict electron densities in agreement with independent determinations of the same, all theories of collision-dominated ionization and recombination start with the supposition that only states below the critical level need be considered in determining the ionization and recombination rates. In principle a finite matrix of transition equations (cut off at the critical state) could be solved simultaneously for the time behavior of the excited-state populations; however, it is expedient and justifiable to consider transitions across all states except one to be very fast in comparison to excitation or de-excitation of that one state. On this basis Bates, et al. (Refs. 7 and 8) computed the rate of populating the ground state by collisional and radiative transitions. Byron, et al. (Ref. 11) have taken the point of view that the critical transition is across the interval between the critical state and the state one principal quantum number below

it (referred to herein as the critical interval). After radiative effects are propely accounted for, their results at high temperature are practically identical with those of Ref. 7. The calculation of Ref. 10 is somewhat different on the surface -- classical ionization rates are summed for all levels below the critical level; however, since the collisional transition cross sections automatically account for all transitions across intervals greater than or equal to the given interval, the various models are in reality equivalent. Differences in the results of these investigators occur, primarily, because of the assumptions made in determining the critical energy level (particularly the manner in which it is influenced by radiative transitions). Lesser differences are related to differences in cross sections used and approximations made in evaluating necessary integrals involving the cross sections.

In formulating the equations of the general model, the present theory follows closely the formulation of Refs. 11 and 12. The point of departure from the Byron model and the primary contribution of the present theory is the development of an explicit analytical procedure for determining the critical energy level.

The cross section for exciting the "jth" state from some other "ith" state by electron collisions is obtained by averaging the individual cross sections over an assumed Maxwell - Boltzmann distribution:

$$\bar{Q}(\epsilon_j - \epsilon_i) = \frac{\int Q(\epsilon_j - \epsilon_i)\ v_e\ f(\vec{v}_e)\ d^3\vec{v}_e}{\int v_e\ f(\vec{v}_e)\ d^3\vec{v}_e} \tag{1}$$

where $f(\vec{v}_e)$ is the Maxwellian velocity distribution function, v_e is the electron speed and $Q(\epsilon_j - \epsilon_i)$ represents the probability that an electron of speed v_e will cause a transition from energy level ϵ_i to ϵ_j. In this equation the thermal speed of the electrons has been factored out of the averaged cross section.

The state notation used is in the fashion of one-electron atoms referenced to ground state so that $\epsilon_o = 0$ refers to the ground state energy (not to be confused with the permittivity of free space), ϵ_i to the energy level one principal quantum number above ground, etc. Because the individual excitation cross sections which will be used later are semiclassical, it must be assumed that transitions from all substates of a given level to some common upper state are equally probable, except for the weighting effect of the degeneracy of each substate: for example, the collisional transition 4P - 5S is twice as probable as the transition 4S - 5S because the P states are twice as degenerate as the S states.

In terms of the averaged cross section, the rate of exciting the "jth" state from all lower states is written as

$$\frac{dn_j}{dt} = n_e \bar{v}_e \sum_{i=0}^{i=j-1} n_i \bar{Q}(\epsilon_j - \epsilon_i) \tag{2}$$

where n_i denotes number density of the "ith" state, n_e denotes electron number density, and $\bar{v}_e$ denotes electron thermal speed.

For the computations to come later, it will be necessary to derive the rate of crossing a given energy level. The convention is now adopted that all cross sections used henceforth represent the probability of exciting transitions across an interval greater than or equal to the given transition interval. The rate of such transitions is related to the cross sections as in Eq. (2), it being understood that the notation refers to crossing the "jth" energy level, not just to exciting the "jth" state.

$$\frac{dn_{j\rightarrow}}{dt} = n_e \bar{v}_e \sum_{i=0}^{i=j-1} n_i \bar{Q}(\epsilon_j - \epsilon_i) \tag{3}$$

$\frac{dn_{j\rightarrow}}{dt}$ means the rate of exciting the "jth" state and all higher states.

In order to evaluate n_i we must assume a Boltzmann distribution below a certain critical state. This assumption is not entirely in accord with experiment. References 10 and 18 show that above the critical state Boltzmann equilibrium between actual states does prevail, the temperature of the distribution being that of the free electrons as determined by use of the Saha equation with the measured free electron and excited-state number densities. Below the critical state the various substates of a given state exist in equilibrium at a temperature between the gas temperature and the free electron temperature. The states themselves are not shown to be in equilibrium by the spectrographic data. Insofar as the effect of this complication of the basic model is concerned, we shall accept, here, the alternatives stated in Ref. 7: either (1) a uniform state distribution is maintained among states below the critical energy level at high plasma density or (2) for a low density plasma in which radiation dominates the problem the state distribution is immaterial. The basic experimental character of the distribution (enhancement of intermediate state populations) is preserved in the model. Figure 1 indicates that, depending on the electron temperature and density, a state in Boltzmann equilibrium with the ground state is, generally, more densely populated than when the same state (as the critical state) is evaluated in Saha equilibrium with the free electrons.

A schematic diagram of the present model is given in Fig. 2. In the equations below, subscript c denotes the critical state and $c - 1$ refers

to the state one principal quantum number below the critical state. From the critical energy level on up to the continuum, all states are in Saha equilibrium with the free electrons; whereas, all states from ground state to the c - 1 state are in Boltzmann equilibrium at the free electron temperature. The energy difference between the states c and c - 1 defines the critical interval $\Delta\epsilon$. In terms of these quantities, the rate of upward crossing the critical level is written below, after substitution of the Boltzmann distribution for states below the critical state.

$$\frac{dn_{c\rightarrow}}{dt} = n_e\, n_{c-1}\, \bar{v}_c \sum_{i=0}^{i=c-1} \bar{Q}\,(\epsilon_c - \epsilon_i)\, \frac{g_i}{g_{c-1}}\, e^{-\frac{\Delta\epsilon}{kT_e}}\, e^{\frac{\epsilon_c-\epsilon_i}{kT_e}} \tag{4}$$

where g_i is degeneracy of the "ith" state, k is Boltzmann's constant, and T_e is the electron temperature.

If there are no opposing transitions, the rate of ionization is just this rate of upward transitions traversing the critical interval. (The neglect of opposing transitions will be examined further in Section V.) Byron's assumption now will be made: the difference between adjacent energy levels is sufficiently small in comparison to the energy level (measured with respect to ground) that the sum in Eq. (2) can be replaced by an integral, the independent variable having been transformed from state index to energy difference between (assumed continuous) states. The result is a general statement of collision-induced ionization.

$$\left(\frac{dn_e}{dt}\right)_{ionization} = \frac{dn_{c\rightarrow}}{dt} = n_e\, n_o\, \bar{v}_e\, \frac{\bar{g}}{g_o}\, \frac{e^{-\frac{\epsilon_c}{kT_e}}}{\Delta\epsilon} \int_{\Delta\epsilon}^{\infty} \bar{Q}_{(E)}\, e^{\frac{E}{kT_e}}\, dE \tag{5}$$

where subscript o denotes ground state and $\bar{g}$ is the average degeneracy of the substates within the critical interval $\Delta\epsilon$.

The collisional recombination expression can be obtained by use of detailed balance, the equilibrium relation being the Saha equation (evaluated at the free electron temperature).

$$\left(\frac{dn_e}{dt}\right)_{recombination} = \left(\frac{h^2}{2\pi\, m_e\, kT_e}\right)^{3/2} \frac{\bar{g}}{g_e\, g_{ion}}\, e^{\frac{\epsilon-\epsilon_c}{kT_e}}\, n_e^{\,2}\, \frac{n_{ion}\, \bar{v}_e}{\Delta\epsilon} \int_{\Delta\epsilon}^{\infty} Q_{(E)}\, e^{\frac{E}{kT_e}}\, dE \tag{6}$$

where m_e is the electron mass, h is Planck's constant, and ϵ is the ionization potential.

Both Eqs. (5) and (6) can be written as a common factor $\mathfrak{F}$ multiplied by the ionization or recombination rate given by the classical Thomson-Bohr theory (see Ref. 4). The classical theory considers a bound state

electron is impulsively excited all the way to ionization by collision with a free electron of appropriate energy. Its results can be expressed as shown below:

$$\left(\frac{dn_e}{dt}\right)_{\substack{\text{ionization}\\ \text{classical}}} = n_e\, n_o\, \bar{v}_e\, e^{-\frac{\epsilon}{kT_e}}\, \sigma_{cl} \tag{7}$$

$$\left(\frac{dn_e}{dt}\right)_{\substack{\text{recombination}\\ \text{classical}}} = \left(\frac{h^2}{2\pi m_e\, kT_e}\right)^{3/2} \frac{g_o}{g_e\, g_{ion}}\, n_e^{\,2}\, n_{ion}\, \bar{v}_e\, \sigma_{cl} \tag{8}$$

where $$\sigma_{cl} = \pi \left(\frac{q_e^{\,2}}{4\pi\, \epsilon_o\, \epsilon}\right)^2$$

q_e is the electronic charge, and ϵ_o is the permittivity of free space.

The ratio of the sequential collision-induced processes to the classical impulsive processes is

$$\Im = \frac{\frac{dn_e}{dt}}{\left(\frac{dn_e}{dt}\right)_{\text{classical}}} = \frac{\bar{g}}{g_o}\, \frac{e^{\frac{\epsilon-\epsilon_c}{kT_e}}}{\sigma_{cl}\, \Delta\epsilon} \int_{\Delta\epsilon}^{\infty} \bar{Q}_{(E)}\, e^{-\frac{E}{kT_e}}\, dE \tag{9}$$

As will be apparent later, $\Im$ varies through many orders of magnitude as the electron temperature ranges between 500 and 3000°K. The computation of ionization and recombination rates from these formal equations depends on the determination of the critical energy level and the average degeneracy of the substates within the critical interval. These problems are considered in detail in the next two sections. The method developed there is, strictly speaking, valid only in the collision-dominated limit, as it ignores the effect of radiative interactions in determining the critical energy level. The equations previously derived, however, are quite generally valid when proper information is supplied concerning the critical energy level.

SECTION III
DEGENERACY OF STATES WITHIN THE CRITICAL INTERVAL

3.1 QUANTUM MECHANICS OF THE ALKALI ATOMS

In this section the quantum mechanical behavior of alkali atoms will be determined in the central force field approximation using a procedure outlined in Fermi's published notes (Ref. 16).

On account of the penetration of the valence electron through the closed shell of inner core electrons, the alkali atom energy levels can be approximately calculated by use of the potential shown below:

$$V_{(r)} = - \frac{q_e^2}{4\pi \epsilon_0 r} \left(1 + \frac{\beta}{r}\right) \tag{10}$$

where r is the radial coordinate for the alkali valence electron. This potential is clearly only approximate. Both the Thomas-Fermi statistical theory (see Ref. 21) and the old quantum theory (see Ref. 22) indicate that an inverse r^4 term occurs because of the polarization of the core electrons by the valence electron at large values of r. The polarization term is replaced, here, by the inverse r^3 term because the latter can be absorbed into the centrifugal portion of the separated Schroedinger equation for radial motion shown below. (See, for example, Ref. 23.)

$$\frac{d}{dr}\left(r^2 \frac{dR}{dr}\right) + \left[\frac{2}{\gamma a_1} + \frac{2r}{a_1} - \ell'(\ell' + 1)\right] R = 0 \tag{11}$$

where

$$\gamma = 2\left[\frac{2\mu_e}{h^2}(\epsilon - \epsilon_{N,\ell})_t\right]^{1/2}$$

μ_e is the reduced electron mass, and a_1 is the first Bohr radius for hydrogen ($h = \frac{h}{2\pi}$). In this equation, ℓ' is an effective angular momentum quantum number; it is not an integer. The relation between ℓ' and ℓ, the ordinary angular momentum quantum number, is

$$\ell'(\ell' + 1) = \ell(\ell + 1) - \frac{2\beta}{a_1} \tag{12}$$

The term β is a constant related to the charge and average radius of the inner electronic core; it need not concern us further. The term γ is the transformed wave number corresponding to the energy eigenvalue. In order to understand the characteristics of the alkali energy levels, let us digress to the hydrogen atom calculation (see Ref. 23).

In the special case of the hydrogen atom, the Schroedinger equation can be transformed by the substitution $x = \gamma r$ with new indices defined as

$$j = \frac{2}{a_1 \gamma} + \ell \quad \text{and} \quad \kappa = 2\ell + 1 \tag{13}$$

The radial equation becomes

$$x \frac{d^2R}{dx^2} + 2\frac{dR}{dx} + \left[j - \frac{\kappa - 1}{2} - \frac{x}{4} - \frac{\kappa^2 - 1}{4x}\right] R = 0 \tag{14}$$

A standard transformation, $R = e^{-\frac{x}{2}} x^{\frac{\kappa-1}{2}} f(x)$, generates the form of the associated Laguerre equation, whose solution is obtained by recognizing that the equation is identical to the result of differentiating the ordinary Laguerre equation κ times with respect to x.

$$x \frac{d^2 f(x)}{dx^2} + \frac{d f(x)}{dx} (\kappa + 1 - x) + (j - \kappa) f(x) = 0 . \tag{15}$$

In terms of the Laguerre functions, the solution of the radial equation for hydrogen is

$$R = e^{-\frac{x}{2}} x^{\frac{\kappa-1}{2}} \frac{d^{\kappa} L_{\gamma}(x)}{dx^{\kappa}} \tag{16}$$

Unfortunately, this straightforward procedure cannot be simply generalized for the case of the alkali potential. Since the differentiation index κ must be an integer, the above procedure cannot be followed when $\kappa = 2\ell' + 1$ is not an integer. In this case the radial solutions could be obtained by numerical integration of Eq. (8); our interest, however, lies only in the dependence of energy levels and degeneracies on ℓ'. These relations can be obtained without having explicit radial solutions.

In analogy to the treatment of the hydrogen atom, let us require that j be a positive integer. If the energy eigenvalues were related to an integral quantum number, the latter would be determined as the principal quantum number $N = j - \ell$. Following Fermi, we define an effective principal quantum number

$$N' = N + \ell - \ell' \tag{17}$$

whose deviation from the integral principal quantum number is the quantum defect δ_ℓ. In terms of these quantities, which characterize the alkali atoms, the energy eigenvalues are written below:

$$\epsilon - \epsilon_{N,\ell} = \frac{\hbar^2}{2 \mu_e a_1 N'^2} \tag{18}$$

where $N' = N - \delta_\ell$

and $$\delta_\ell = \ell' - \ell = \left[\left(\ell + \frac{1}{2}\right)^2 - \frac{2\beta}{a_1}\right]^{1/2} - \left(\ell + \frac{1}{2}\right)$$

Since the treatment of the alkali atoms used here assumes a central force for the field in which the valence electron moves, the simple degeneracy of a given substate is $2(\ell + 1)$; when the angular momentum

caused by electron spin is added, the degeneracy becomes $2(\ell+1)$. Now that the degeneracies and energy levels of the alkali atoms have been related to appropriate quantum numbers, defined in such a way as to collapse the alkali quantum mechanics to hydrogen-like description, the average degeneracy of the substates in the critical interval can be calculated. The derivation is given in the next section.

3.2 AVERAGE DEGENERACY APPROXIMATION

In this section the average degeneracy for states within the critical interval is computed to the first order in terms of $\frac{1}{N'}$. By means of the approximation scheme of this section, the degeneracy and subsequently, the critical energy level, are related to known parameters characterizing the alkali atoms. The order of approximation introduced here will be followed in determining the final ionization and recombination rates, so that the present theory is formally restricted to first order terms in the reciprocal of the critical quantum number.

The derivative of the quantum defect is obtained from Eq. (18):

$$\frac{d\delta_\ell}{d\ell} = -\frac{\delta_\ell}{\delta_\ell + \ell + \frac{1}{2}}.$$

The simple degeneracies are now averaged over the energy levels corresponding to substates within the critical interval to obtain the average degeneracy $\bar{g}$. In terms of the integral below, $\bar{g}$ can be written as

$$\bar{g} = \frac{2(N_c' - 1)^2 N_c'^2}{2N_c' - 1} I \tag{19}$$

where

$$I = 2\left| \int_{\ell=0}^{\ell=\ell_M} \left(\frac{1+\ell}{N'^3}\right) dN' \right| = \left| \frac{1}{(N_c' - 1)^2} - \left(\frac{1+\ell_M}{N_c'^2}\right) + \int_{\ell=0}^{\ell=\ell_M} \frac{d\ell}{(N - \delta_\ell - 1)^2} \right|$$

In this derivation ℓ_M denotes the maximum value of ℓ in the critical interval. It should be noted that the integration begins at some initial value of ℓ with the principal quantum number equal to $N_c - 1$. As ℓ increases to ℓ_M the effective principal quantum number is considered to change from $N_c' - 1$ to N_c'; whether an S state is crossed is immaterial because $N - \delta_{\ell_m} \simeq N - \delta_0 + 1$. The last term in Eq. (19) is evaluated by use of Eq. (18), yielding

$$\bar{g} = \frac{2N_c'(N_c' - 1)}{(2N_c' - 1)} \left\{ \left(1 + \frac{1}{\alpha}\right)\left(N_c' - 1\right) - \frac{N_c'^2}{N_c' - 1} + N_c'(N_c' - 1) \int_{\ell=0}^{\ell=\ell_M} \frac{\ell + \frac{1}{2}}{\delta_\ell (N' - 1)^2} d\delta_\ell \right\} \tag{20}$$

The integral term can be shown by use of a second order Maclaurin expansion of δ_ℓ to be a second order term in $\frac{1}{N_c'}$. With only first order terms retained, the degeneracy assumes the form shown in Eq. (21).

$$\bar{g} = \frac{2N_c'(N_c' - 1)}{(2N_c' - 1)}\left[\frac{1}{a}(N_c' - 1) - 1\right] \tag{21}$$

where $$a = \frac{N_c'}{1 + \ell_M},$$

For comparison, the corresponding degeneracy for hydrogen is shown as Eq. (22):

$$\bar{g}_M = (N_c - 1)^2 \tag{22}$$

Since $\ell_M \to N_c - 2$ for hydrogen-like states, a varies from one in the limit of very high quantum number to $\frac{1 + N_o'}{1 + \ell_M}$ for the lowermost states. It will be apparent in the next chapter, however, that the critical energy level is quite insensitive to the form of the degeneracy in the high quantum number (low temperature) limit. Because of this fact, the alkali atom behavior can be adequately characterized, in the present theory, by the low quantum number limit; henceforth, a will be taken to be its lower limit value, $a = \frac{1 + N_c'}{1 + \ell_M}$, where N_o' refers to ground state, effective, principal quantum number.

SECTION IV
LOCATION OF THE CRITICAL STATE

As Byron, et al. (Ref. 11) have indicated, the critical state is located so that the rate of transition across the critical state corresponds to the slowest in a sequence of transitions from ground state to the continuum. This minimal transition is affected by both the balance of collision-induced excitation and de-excitation and the interaction of collisional and radiative transitions. In this section the radiative effects are ignored and the rate of transition across the critical state with respect to the critical quantum number is formally minimized, making use of the parameters introduced in the preceding section. The general equation for determining the critical quantum number is shown below:

$$\frac{d}{dN_c'}\left(ln\ \frac{dn_e}{dt}\right) = \frac{d\ ln\ \bar{g}}{dN_c'} + \frac{d\ ln\ F\left(\frac{\Delta\epsilon}{kT_e}\right)}{dN_c'} - \frac{1}{kT_e}\frac{d\epsilon_c}{dN_c'} - 2\frac{d\ ln\ \Delta\epsilon}{dN_c'} = 0 \tag{23}$$

where

$$F\left(\frac{\Delta\epsilon}{kT_e}\right) = \frac{\Delta\epsilon}{\epsilon^2 \sigma_{c1}} \int_{\Delta\epsilon}^{\infty} \bar{Q}_{(E)} \; e^{\frac{E}{kT_e}} \; dE \tag{24}$$

To solve this equation, let us use the Gryzinski (Ref. 9) cross sections for collision-induced excitation, as linearized by Byron, et al. (Ref. 12). The various cross sections will be considered in more detail in a later section. The parameters to be inserted into Eq. (23) are listed below:

$$\frac{d\ ln\ \bar{g}}{d\ ln\ N_c'} = \left(\frac{N_c'}{N_c' - 1}\right)\left[\frac{2N_c' - (a+2)}{N_c' - (a+1)}\right]$$

$$\frac{d\epsilon_c}{dN_c'} = 2\epsilon \; \frac{N_o'^2}{N_c'^3}$$

$$\frac{d\ ln\ F\left(\frac{\Delta\epsilon}{kT_e}\right)}{d\ ln\ N_c'} - \frac{\left(\frac{d\ ln\ \Delta\epsilon}{d\ ln\ N_c'}\right)}{\left(1 + \frac{\Delta\epsilon}{kT_e}\right)} \tag{25}$$

$$\frac{d\ ln\ \Delta\epsilon}{d\ ln\ N_c'} = -\frac{2}{(N_c' - 1)}\left[\frac{3N_c'(N_c' - 1) + 1}{2N_c' - 1}\right]$$

At this stage it is advantageous to split the critical quantum number according to the following transformation:

$$\frac{1}{N_c'} = \xi\zeta, \quad \xi^2 = \frac{kT_e}{N_o'^2 \epsilon} \quad \text{and} \quad \zeta^2 = \frac{\epsilon - \epsilon_c}{kT_e}$$

The two new parameters ξ and ζ are of direct physical interest; ζ^2 is proportional to the shift of the critical energy level down from the ionization potential, and ξ^2 is the dimensionless free electron mean energy. The normalizing factor in the expression for ξ^2 is related to the Rydberg constant for the element in question. The normalization has the effect of removing any dependence on atomic mass, so that the true effect of differences in atomic structure can be ascertained. In terms of these quantities and to the first order approximation with respect to $\xi\zeta$, the equation finally determining the critical energy level is written below as a simple quadratic:

$$\zeta^4 + \frac{\zeta^2}{2}\left(\frac{1}{\xi\zeta} - y\right) - \frac{X}{2\xi\zeta} = 0 \tag{26}$$

where

$$X = \frac{1}{2}\frac{d\ ln\ \bar{g}}{d\ ln\ N_c'} + \frac{9}{2 - \xi\zeta}$$

and

$$y = \frac{d\ ln\ \bar{g}}{d\ ln\ N_c'} + \frac{6}{2 - \xi\zeta}$$

The solution to this equation is presented in Fig. 3. The temperature ranges from zero to about 2500°K. The present theory apparently compares favorably (within about 10 percent at high temperature) with the specific determinations of Ref. 12. From quantities stated in Eq. (25), one can see that at high critical quantum numbers, the degeneracy derivative is essentially hydrogen-like and is independent of α. This behavior accounts for the previous remark that the lower limit of α is sufficient to characterize the behavior of the various one-electron substances. As is apparent in Fig. 3, the theory and Byron's points converge to hydrogen-like behavior at the high quantum number (low temperature) limit. It is noteworthy, however, that at the upper end of the curves, where the discrepancies between theory and Byron's points occur, the disparity exists for hydrogen (whose degeneracy is exact) as well as for the alkalies. The reason for this discrepancy is the order of approximation inherent in Eq. (26). In this equation consistency with the order of approximation in the degeneracy computation has been maintained because inclusion of second order terms in Eq. (26) (with only first order terms in the degeneracy) leads to a rapid divergence of ζ. Consistent inclusion of second order terms in both the degeneracy and the determination of the critical state should alleviate this discrepancy; however, such additional and arduous mathematical labor is not worthwhile because error in determination of the critical energy level propagates into the final ionization and recombination rates only as the square of the relative error in $\epsilon_{c'}$. It should be noted, however, that errors in the degeneracy propagate linearly into the final rate expressions. The significance of these errors in the approximations will be more fully explored in Section V.

Before turning to the final computation of the ionization and recombination rates, it is of some interest to compare various estimates of the critical energy level behavior. The present results indicate approximately $\frac{N_c'}{N_o'} = \left(\frac{\epsilon}{5\ kT_e}\right)^{1/2}$: whereas, Hinnov and Hirschberg (Ref. 10) found $\frac{N_c'}{N_o'} = \left(\frac{\epsilon}{kT_e}\right)^{1/2}$.

This apparent discrepancy can be explained on the basis of radiative transitions across the critical interval. Hinnov and Hirschberg determined the critical state (for electron mean energy $\leq \frac{1}{4}$ ev) by equating forward and reverse transitions across the critical interval, requiring Boltzmann equilibrium between the states c and $c-1$, and using very high critical quantum number approximations to solve the resulting transcendental equation for N'_c. These assumptions are inconsistent with those of the present model, wherein the critical state is assumed in Saha equilibrium with the free electrons and the very high quantum number approximation is not appropriate.

The Hinnov and Hirschberg critical state calculation actually corresponds to assuming collision-induced transitions up to and across a radiation-limited critical interval. It is applicable whenever radiation is the predominant mechanism of crossing the critical interval; this predominance occurs late in the afterglow and corresponds in their experiment to electron mean energy $< \frac{1}{4}$ ev. Above this energy the free electron density is sufficient to maintain a collision-limited critical state, and Hinnov and Hirschberg use a different formula (accounting for both collision-induced and radiative transitions between specified states) proposed in Ref. 6 and repeated in Ref. 10. This calculation agrees numerically with the present theory and their spectroscopic data (2^3p-N^3D lines in helium), yielding the critical quantum number $N_c' = 4$. Below $\frac{1}{4}$ ev, their low temperature formula overestimates and the present theory underestimates the critical quantum number. In this region the critical quantum number is best estimated by two other theories. Both a simple calculation by Ref. 11 and a much more elaborate one quoted in Ref. 24 give $N_c' \approx \left(\frac{\epsilon}{3kT_e}\right)^{1/2}$, lying between the present results and those of Ref. 10.

In summary of these results, one can say that the present theory and the numerical points of Ref. 12 underestimate the critical quantum number whenever radiative effects are important. Although such radiative predominance can often occur in hydrogen and helium laboratory plasmas, it is most uncommon in alkali-seeded plasmas, so that the present theory provides a good description for plasmas of interest in practical MHD devices.

To date there have been no experimental determinations of the critical level with the exception of the previously mentioned spectroscopic studies. Observation of the time variation of various spectral line intensities coupled with measurements of electron temperature and density variation and comparison with theoretical calculations should provide a more definite determination of the critical level behavior, if such is needed. This possibility is considered in Section VII.

SECTION V
FINAL COLLISIONAL IONIZATION AND RECOMBINATION RATES

5.1 GENERAL THEORY

Now that the critical energy level behavior has been determined, the collisional ionization and recombination rates can be determined from Eqs. (5) and (6). Since the factor $\mathfrak{F}$ is common to both the ionization and recombination rates, only $\mathfrak{F}$ will be formally considered here. In order

to simplify the computation of $\Im$ in a fashion consistent with the determination of the average degeneracy $\overline{g}$, one must determine the minimum quantum number consistent with the first order approximation (in terms of $\frac{1}{N_c'}$) inherent in $\overline{g}$. Higher order terms can be eliminated from consideration in $\Im$ by using the criterion developed.

The basic inequality expressing the limit of the first order degeneracy approximation is

$$\frac{1}{(N_o'-1)^2} < \left| \frac{1}{N_c'-1} - \frac{1}{N_c'}\left(1 + \frac{1}{\alpha}\right) \right| \tag{27}$$

This inequality imposes the following restriction on the value of the critical quantum number:

$$\xi\zeta < \left| \left[\alpha\left(1 + \frac{\alpha}{4}\right)\right]^{1/2} - \left(1 + \frac{\alpha}{2}\right) \right|$$

or (28)

$$N_c' > \left| \left[\alpha\left(1 + \frac{\alpha}{4}\right)\right]^{1/2} - \left(1 + \frac{\alpha}{2}\right) \right|^{-1}$$

These limits of the mathematical approximations also agree approximately with the actual quantum numbers for the states one principal quantum number above ground: for cesium the mathematical limit is 2.63 and the actual quantum number is 2.93; for potassium the mathematical limit is 3.12 and the actual quantum number is 2.93. It is thus apparent that for potassium the limit of validity of the mathematical approximations is reached shortly before the critical level has lowered to the level one principal quantum number above the ground state; whereas, for cesium, the mathematical approximations are adequate at the physical limit.

For both these elements the assumptions of the theory actually become invalid when the critical state approaches the limit mentioned. Specifically, the assumption of equal transition probability (except for degeneracy) for transitions originating from the various substates and crossing the critical state becomes quite questionable on account of the large differences in spacing of the substates which constitute the interval between the ground state and the state one principal quantum number above ground. The procedure adopted here is to calculate the specific limit of $\Im$ associated with the critical state fixed at the state one principal quantum number above ground. Two extremes of the degeneracy are assumed

corresponding to the assumption that (1) the only transition of importance is that originating at the ground state and (2) transitions originating from all states within the interval are equally important. The letter assumption produces transition rates somewhat larger than the former. Presumably, if the correct distribution of transitions were known (from a quantum mechanical calculation of transition probabilities) the associated transition rates should at some temperature be tangent with an extrapolation of the original theory into regions where it is in doubt.*

With all these restrictions in mind, let us now write the form of $\Im$ consistent with the physical limitations of the model as below:

$$\Im = \frac{1}{8} \frac{\left(1 - \frac{5}{2}\xi\zeta\right)}{\left(N_o' \xi^2 \zeta^2\right)^4} \left[\frac{1}{a} - \xi\zeta\left(1 + \frac{1}{a}\right)\right] e^{\zeta^2} F\left(\frac{\Delta\epsilon}{kT_e}\right) \tag{29}$$

and

$$\Im_{Limit} = \left(\frac{\epsilon}{\epsilon_1}\right)^2 e^{\frac{\epsilon-\epsilon_1}{kT_e}} F\left(\frac{\epsilon_1}{kT_e}\right) \frac{\bar{g}}{g_o} \tag{30}$$

where ϵ_1 is the energy level of the state one principal quantum number above ground.

5.2 COLLISIONAL EXCITATION CROSS SECTIONS

Presently, there exists no completely satisfactory method for determining collision-induced transition probabilities. According to Ref. 25, quantum theory is capable of treating this problem exactly; however, the difficulty of the mathematics involved has prevented the successful exploitation of quantum mechanical techniques for all but the simplest systems. Even for hydrogen the Born approximation predicts low energy results which overestimate experimental results by about an order of magnitude; at high energies the two agree fairly well, as would be expected according to the nature of the Born approximation. Various additional sophistications (such as inclusion of exchange effects and consideration of coupling of states) have lowered the cross section somewhat, at the expense of such mathematical complexity that extension to more complicated systems than hydrogen is most unlikely. Omidvar (Ref. 26) has developed a procedure (using the electronic computer) for calculating elastic and inelastic cross sections in hydrogen. His results lower the theoretical cross sections (from the Born value) to values in agreement with the experiments of Ref. 27 but considerably

*The author acknowledges Dr. L. Ring for the demonstration of this point.

higher than those of Ref. 28. He indicates that inclusion of two more states in the coupling consideration (he considered four) will reduce the results about 30 percent. Although these theoretical trends are, clearly, in the right direction, understanding of collision-induced transitions is far from complete -- one unexpected difficulty being the lack of agreement of the experiments mentioned.

In an effort to extract some information concerning quantum mechanical peculiarities of the problem without actually solving it, Seaton (Ref. 25) has assumed the collisional excitation process involves emission and reabsorption of a virtual photon. From this model he has shown the collisional transition probability for optically allowed transitions to be proportional to the oscillator strength for the analogous optical transition; hence, one may expect some sort of selection rule to govern collisional transitions, just as is true for radiative transitions.

In the absence of such selection rules, one can only use classical cross sections, assuming the most probable transition is that for which $\Delta \ell = 0$ and partially accounting for the other transitions (across smaller intervals than the primary one just mentioned) by assigning them the same a priori probability, except for the weighting effect of the various degeneracies. Still, one must choose a cross section for the lumped transitions.

Gryzinski (Ref. 9) has considered classical collisions between free electrons and bound state electrons moving in allowed orbits and with velocities compatible with quantum mechanical limitations. His cross sections have been evaluated by Kingston (Ref. 29) for hydrogen and compared with various similar approximations, experimental data (directly obtained from ionization experiments and indirectly, by comparison of collisional-radiative recombination theory with experiments in hydrogen and helium) and the Born approximation. He concludes that the cross sections for ionization are accurate within about 20 percent; whereas, those for excitation are good within at least a factor of two. At high energy, the classical theory underestimates the Born results, because the quantum theory effectively considers impact parameters extending to infinity. The Born cross section falls off as $\frac{1}{E}(ln\, E)$ at large energies; the classical cross section goes as $1/E$. At low energies, classical theory overestimates reality somewhat,, because classical theory assumes the excitation probability is one whenever the impact parameter of the incoming electron lies within a specified range (see Ref. 25). In this respect the cross sections in Ref. 9 are superior to those of the Thomson-Bohr (see Ref. 4) theory because the averaging over all locations of the bound electron has the effect of "smearing out" the impact parameter in a fashion reminiscent of quantum mechanics. (The Thomson-Bohr theory represents the limiting case of Gryzinski's theory when the energy of the bound electron is zero.)

Gryzinski (Ref. 9) writes the cross section for excitation of a bound state electron with energy E_1 through an interval E by collision with an electron of energy $\frac{m_e v_e^2}{2}$ as

$$Q(E) = \pi \left(\frac{q_e^2}{4 \pi \epsilon_o E} \right) g_j \tag{31}$$

where g_j is a function of the colliding electron energy, the bound electron's initial energy, and the transition interval. This function is plotted in Fig. 4. Because of the difficulty of integrating this function over a Maxwell-Boltzmann distribution of electron velocities, Byron, et al. (Ref. 12) use a linear approximation to the first part of the Gryzinski curves, the slope being a weak function of the electron energy on account of the dependence of the bound electron's initial energy on free electron energy. A different procedure is used in the present calculations; because the Thomson-Bohr cross sections can be easily integrated over a Maxwell-Boltzmann distribution, these cross sections are adjusted by a factor of 0.8 to bring them into approximate agreement with the low energy portion of the curve marked $E_1/E = 1$. The high energy portion of these curves is now underestimated; however, the exponential tail of the Maxwellian distribution will suppress these high energy transitions, so that the effect should not be noticeable. This treatment probably underestimates the transition probabilities for high quantum number, but certainly by less than a factor of two. Indeed the final results at low temperature agree well with both experiments and other theories, as will be apparent shortly.

In the equations below the Thomson-Bohr cross sections and the linearized Gryzinski cross sections are stated and integrated over a Maxwell-Boltzmann distribution:

$$Q_{T-B}(v_e) = \pi \left(\frac{q_e^2}{4 \pi \epsilon_o} \right)^2 \left(\frac{2}{m_e v_e^2} \right) \left(\frac{1}{E} - \frac{2}{m_e v_e^2} \right)$$

and

$$\bar{Q}_{T-B}(E) = \sigma_{cl} \left(\frac{\epsilon}{kT_e} \right)^2 \left[Ei \left(\frac{E}{kT_e} \right) - \frac{kT_e}{E} e^{-\frac{E}{kT_e}} \right] \tag{32}$$

where $$Ei(V) = \int_{\cdot}^{\infty} \frac{e^{-u}}{u} du$$

$$\bar{Q}_G(E) = \sigma_{cl} \left(\frac{\epsilon}{E} \right)^2 B e^{-\frac{E}{kT_e}} \left[1 + \left(\frac{2kT_e}{E} \right) \right] \tag{33}$$

where B is Byron's dimensionless slope of Gryzinski's function g_j. The cross-section integrals $F\left(\frac{\Delta\epsilon}{kT_e}\right)$ are now determined for the preceding cross sections:

$$F_{T-B} = 0.8 \left(\frac{\Delta\epsilon}{kT_e}\right) e^{\frac{\Delta\epsilon}{kT_e}} Ei\left(\frac{\Delta\epsilon}{kT_e}\right) \tag{34}$$

and

$$F_G = B\left(1 + \frac{kT_e}{\Delta\epsilon}\right) \tag{35}$$

All pertinent quantities having been determined, we can now calculate the ionization and recombination rates from $\Im$ (determined by Eqs. (26) and (29) or (30) and the relations for ionization and recombination coefficients stated below:

$$K_{ionization} = \sigma_{cl} \bar{v}_e e^{-\frac{E}{kT_e}} \Im$$
$$\frac{dn_e}{dt} = n_e n_o K_{ionization} \tag{36}$$

$$K_{recombination} = \left(\frac{h^2}{2\pi m_e kT_e}\right)^{3/2} \sigma_{cl} \frac{g_o}{g_e g_{ion}} \tilde{v}_e \Im$$
$$\frac{dn_e}{dt} = n_e^2 n_{ion} K_{recombination} \tag{37}$$

In the following section, recombination coefficients computed by use of the modified Thomson-Bohr cross section are discussed. Though they are not presented, results obtained from the linearized Gryzinski cross sections are almost identical.

5.3 COLLISIONAL RECOMBINATION RESULTS

The final results of the collision-induced recombination study are presented in Fig. 5 as the variation with electron temperature of the effective three-body recombination coefficients. Only hydrogen, cesium, and potassium have been considered because the behavior of lithium and sodium is expected to resemble that of potassium; similarly, cesium and rubidium should recombine at about the same rate.

One notices immediately that the various theories for different elements agree within the resolution of most present-day experiments at low temperatures; however, at high temperatures there is considerable

divergence. The basic differences between the theories of Refs. 11, 12, and the present author are related to the first order approximation for finite critical quantum number effects inherent in the present theory. In turn, all these theories differ from that of Ref. 10 by the basic differences in the computation of the critical quantum number. The present theory, in particular, computes hydrogen recombination rates at high temperature an order of magnitude less than the work of Ref. 10.

The present results agree well with the theoretical studies of cesium reported by Dugan (Ref. 17) which came to the author's attention after completion of the present study. Dugan's calculation extends to 10, 000°K. Because his method of determining the critical state (by means of the spectral data and the use of an electronic computer) does not exclude the collapse of the critical interval into transitions which violate $\Delta \ell = 0$, Dugan's calculations include contributions from critical states lower than the state one principal quantum number above ground. Consequently, his high temperature results are somewhat higher than those of the present theory. At the other end of the temperature scale Dugan's results are, generally, slightly lower than those of the present theory because he includes forward as well as reverse transitions across the critical state. In the present theory the tendency to overestimate the net transition rate because of neglect of opposing transitions is partially compensated by the underestimation of the collision cross section for transitions between high quantum number states mentioned in the previous section. At any rate, for most of the temperature range shown Dugan's numerical solutions and the present calculations are practically indistinguishable.

Some confirmation of the present results can be obtained from the recombination experiments of Refs. 19 and 20 in near thermal cesium plasmas and Ref. 30 in potassium-seeded argon. The data of Harris (Ref. 20) are not shown in the figure because Harris included an empirical correction for ambipolar diffusion and molecular ion dissociative recombination. He added corrections for these effects to recombination mean free times obtained from the theory of Ref. 10; the results agreed well with the experimental measurements for electron densities greater than 5×10^{12}/cc. Below this density he found faster recombination than that predicted by theory. In these experiments the electron temperature range was from 1250 to 1700°C. In this range the present theory for cesium agrees with the calculation of Ref. 10 for hydrogen within about 20 percent--far within the experimental inaccuracy. This agreement with the experimental data of Ref. 20 is regarded as a sensitive test of the present method of determining the critical energy level at electron temperatures less than 2000°K.

At high temperatures, where the finite quantum number effects become appreciable, the present theory for cesium agrees fairly well with the data of Ref. 19; however, the density dependence (resulting from radiative effects) of these experiments produces sufficient scatter in the data that conclusive comparison is not possible at this stage. Radiative effects in a collision-dominated plasma will be accounted for in the next section, and further comparison of experiment and theory must await development of these effects.

The data of Ref. 30 (which is quite a recent publication) show considerable scatter; however, the results generally confirm the theoretical predictions. The numerical computations of Byron et al. (Ref. 12) more nearly fit the average of the data than do the present results because of inaccuracies in the degeneracy approximation to be discussed below. The theoretical uncertainties, nevertheless, are well within the experimental scatter.

As the critical state approaches the state one principal quantum number above ground, the recombination coefficient assumes the limiting form discussed earlier. Such a transition is quite evident in the cesium curve. Extrapolation of the original curve provides a reasonable estimate between the two lower limit curves shown. In the case of potassium, the mathematical assumptions in the degeneracy approximation fail before the physical limit is reached, and the high temperature portion of the curve underestimates the lower limit considerably on account of the progressive deterioration of the degeneracy approximation. It can be shown that the smaller α is, the better is the approximation for $\bar{g}$. Since cesium includes the 5D states in the interval between ground state and the state one principal quantum number above ground and the potassium lowermost critical interval has no such D states, $\alpha_{cesium} < \alpha_{potassium}$; hence the degeneracy approximation for cesium remains good after the potassium approximation has failed. Physically, the presence of the D states also means that the lower limit curve for cesium marked "all transitions" is more appropriate than the lower limit curve marked "primary transition" in describing the high temperature behavior of cesium recombination. The trend of the extrapolated curve agrees with this observation.

SECTION VI
RADIATIVE CONSIDERATIONS AND FINAL COMPARISON BETWEEN EXPERIMENTS AND THEORY

Although the problems of interest in this study are primarily concerned with collisional effects, it is necessary to consider the implications

of radiative-collisional interaction over a range of optical opacities before the final comparison of theory and experiment can be made. In addition to the small direct effect of radiative recombination (or photo-ionization), the ionization and recombination rates are affected by the influence of radiation on the distribution of excited states (hence, the location of the critical state). In addition, one may question the effect of additional cascading between lower states resulting from radiation. (This effect has been taken into account in the second calculation for hydrogen at high electron temperatures in Ref. 10.)

The assumption of Boltzmann equilibrium between states lower than the critical state is equivalent to an infinite rate of cascading (up and down) so that, within the context of the present theory, the effect of line radiation can be considered only to the extent of its effect on the location of the critical state and the enhancement of transitions across the critical interval. It should be noted that if the plasma were optically thick to all line radiation, a Boltzmann distribution of lower states would be assured on account of the mutual requirements implied by blackbody radiation; the balance between absorption, induced emission, and spontaneous emission; and thermal equilibrium between excited states and the radiation field. Similarly, in the limit of collision domination, thermal equilibrium between free electrons and valence electrons implies a quasi-equilibrium distribution of states, if the free electrons undergo sufficient elastic collisions to maintain a Maxwell-Boltzmann distribution of free electron speeds. (This point is mentioned in Refs. 7 and 8 and in Ref. 31 in a discussion of local thermodynamic equilibrium.)

The effect of line radiation in determining the distribution of states and the critical state location can be assessed by comparing radiative and collisional transition probabilities across the critical interval. Since the collisional transitions considered in this report correspond to optically forbidden single transitions, the competition between collisions, two stage allowed radiative transitions across the same interval as the collisions, and optically allowed single transitions across some interval nearly equal to the collisional interval must be considered. Since the line intensities are usually represented by the Einstein transition probabilities per unit time, the relative effectiveness of radiation versus collisions can be represented as the quotient of the radiative transition probability per unit time and the collisional transition probability per unit time. For the sake of convenience, it will be assumed that all transitions crossing a given critical interval are equally energetic but differ in probability on account of having different oscillator strengths. The composite oscillator strength for a dual transition will be defined as the square root of the product of oscillator strengths for the individual transitions. The oscillator strength for all transitions across a given critical interval will be computed by

summing the oscillator strengths for all complete transitions across that interval. The necessary mathematical relations for computing these effects are written below.

The Einstein transition probability coefficient for emissive transitions across the critical interval is obtained from Ref. 32 in Kramers' form (the Gaunt factor is taken to be one):

$$A_{c,\,c-1} = 8(\pi)^{3/2} \frac{g_{c-1}}{g_c} \frac{\sqrt{\sigma_{c1}}\,\epsilon^2}{m_e\, c^3} \nu_{c,\,c-1}^2\; f_{c,\,c-1} \tag{38}$$

where $\nu_{c,\,c-1} = \frac{\Delta\epsilon}{h}$ is the frequency of the transitions across the critical interval, c is the speed of light, and $f_{c,c-1}$ represents the composite oscillator strength for all possibilities of emissive crossing the critical interval. The analagous collisional transition probability (per unit time) is

$$\frac{1}{n_{c-1}} \frac{dn_c}{dt} = n_e\, v_e\, \sigma_{c1} \left(\frac{\epsilon}{\Delta\epsilon}\right)^2 \frac{\bar{g}}{g_{c-1}}\, e^{-\frac{\Delta\epsilon}{kT_e}}\, F\left(\frac{\Delta\epsilon}{kT_e}\right) \tag{39}$$

The ratio of radiative to collisional transitions is obtained from Eqs. (38) and (39) after use of Boltzmann's and Saha's relations:

$$\chi = \frac{(2\sqrt{\pi})^3}{n_e} \frac{g_{c-1}}{\bar{g}} \frac{(\Delta\epsilon)^4}{m_e\, c^3\, h\, \bar{v}_e\, \epsilon \sqrt{\sigma_{c1}}}\, F\left(\frac{\Delta\epsilon}{kT_e}\right) f_{c,\,c-1} \tag{40}$$

It is the same for both excitation and de-excitation.

Table I shows the compilation of oscillator strengths for crossing various critical intervals. These results presented in Ref. 33 for cesium are only approximate and caution must be exercised in applying them because the Thomas-Kuhn sum rule (see Ref. 21) is occasionally violated unavoidably. The oscillator strengths whose values are listed as 1+ were quoted as greater than one in the original article.

Table II shows the values of χ obtained from the quoted oscillator strengths and Eq. (40). It is apparent that radiative transitions outweigh collisional crossing of the interval between ground state and the state one principal quantum number above ground; whereas, collisional transitions are more important than radiation in crossing higher critical intervals. Calculations in Ref. 34 indicate that for transitions from excited states to ground most laboratory plasma are optically thick, except for the (Doppler and pressure broadened) wings of the resonance lines. On the basis of those results it will be assumed in the present computation that excited state to ground transitions are completely absorbed and that other line transitions represent small perturbations of the collisional transition rate.

The enhancement of recombination by line radiation is ultimately computed by multiplying the collisional results by $1 + \chi$. When these computations are compared with the experimental data of Ref. 19 an unexpected difficulty is encountered: at about 2300°K the critical state is 8 S; the next higher critical state 8 P occurs at about 1900°K. Since the range of the data of Ref. 19 is $2000°K \leq T_e \leq 2320°K$, it is evident that some mixing of critical states must occur at the intermediate temperatures. Equal sharing would mean that 2100°K should be the dividing line between temperatures associated with the two critical states. Since the transitions associated with the 8 P critical state are about three times more probable than those across the 8 S critical state at their respective temperatures, the line of demarcation will arbitrarily be placed at 2200°K. For temperatures above 2200°K, the critical state is taken to be 8 S, for temperatures below 2200°K, the critical state is taken to be 8 P. Although this oversimplification merely specifies the range over which each of the two critical states predominates, rather than considering the mixing of critical states at a given temperature, the procedure does provide a guideline for estimating radiative enhancement for cesium recombination rates.

Figure 6 shows the final comparison of the present theory with the available experiments. The straight lines represent collisional theory without radiative effects. In the radiative computation direct radiative recombination has been ignored, as it is nearly constant over the temperature range and on the order of 10^{-12} cm^3/sec. Considering the scatter of the data, the agreement between theory and experiment is satisfactory; moreover, within the uncertainties present, purely collisional theory provides a good description of the recombination process.

SECTION VII
CONCLUDING REMARKS

This report has presented a theoretical study of ionization and recombination in alkali plasmas having electron densities of 10^{12} - 10^{15} electrons/cc. The transition model used assumes the existence of a critical state in equilibrium with free electrons. The net ionization or recombination rate is equal to the transition rate across the critical interval defined by the critical energy level and the level one principal quantum number below it.

The primary contribution of this investigation has been the determination of the critical energy level behavior (with respect to electron temperature). From an approximate quantum mechanical description of the alkali

atom as one electron revolving in a (first order) noncoulombic central force field, the energy level, quantum defect, and simple degeneracy of a given substate have been related to the quantum numbers ℓ and N. The average degeneracy of substates within the critical interval has been determined from these relations to first order in 1/N. By using the energy levels and average degeneracies computed in this way, the ionization and recombination rates have been minimized with respect to the critical energy level. The resulting expressions permit determination of the critical state for any (effective) one-electron atom whose ionization potential, effective ground state quantum number, and maximum orbital quantum number in the interval between ground state and the state one principal quantum number above ground are known. This procedure contrasts with Byron's method of determination of the critical state. In the latter, energy levels and degeneracies of all states of interest must be used in a graphical procedure which must be repeated for each separate electron temperature. The critical states of the present theory agree within 10 percent with Byron's.

Using the analytical expressions developed for the critical state behavior, the collisional recombination coefficients for hydrogen, cesium, and potassium have been presented for electron temperature ranging to 3500°K. Within the resolution of present-day experiments, the basic theory is well confirmed. Comparison with other theories and evaluation of the limits of validity of the mathematical approximation indicates, however, that for sodium, lithium, and potassium the present theory underestimates recombination rates at high temperature by about 50 percent (well within the experimental resolution); whereas, for cesium and rubidium, the present approximations are quite adequate. Since the present theory represents, to the author's knowledge, the only analytical study of alkali collisional ionization and recombination to date (the other theories are numerical in character), it has the merit of providing a simple description of the ionization-recombination process for any atom whose quantum mechanical structure can be reduced to an effective one-electron description. In addition to this inherent simplicity in calculation, the present theory advantageously incorporates the effect of different atomic structure of the elements under consideration through the dependence of the critical energy level on the simple parameter a. This theory is easily generalized through use of the methods of Section VI to include radiative effects, provided radiative transitions are not the dominant mode for traversing the critical interval. For collision-dominant conditions, the present theory is accurate within (at worst) 50 percent. For radiation-dominant conditions the Hinnov and Hirschberg theory is more applicable than either the present theory or the various forms of the Byron theory.

At present, truly definitive experiments concerning ionization and recombination in collision-dominated alkali plasmas do not exist. Within the resolution of present-day experiments (factor of two), the general theoretical model is well confirmed. An additional test of the model can be obtained by comparing experimentally observed relaxation in streaming plasmas subjected to a constant electric field with theoretical predictions.

A computer program is being developed at AEDC whereby the nonlinear electron equations of motion can be solved numerically, using the ionization and recombination theory developed in this report. Such a procedure has the advantage that it not only produces relaxation profiles of electron temperature and number density (to be compared with experimental data), but also yields the theoretical time variation of the critical state, which can be compared with time-resolved spectra. The disadvantage of this procedure is relative insensitivity of the results to the ionization and recombination cross sections, complicated by the lack of precise knowledge of possible electron energy losses within the plasma.

Within the restrictions imposed by these ambiguities, preliminary results of the calculations indicate that the experimental data in Ref. 35 on relaxation of a potassium-seeded argon plasma can be fairly well corroborated with theory.

More refined experiments along the lines of interest of the present study should ideally include both electrodynamic and spectral measurements at various locations along a channel through which a high-speed (1000 m/sec) low temperature (2000°K or less) alkali-seeded plasma is flowing. In order to avoid low electron density difficulties the electric fields imposed should be at least 10 v/cm. Visible radiation should be monitored at least every 5 cm.

REFERENCES

1. Massey, H. S. W. and Burhop, E. H. S. Electronic and Ionic Impact Phenomena. Oxford University Press, London, 1952.

2. D'Angelo, N. "Recombination of Ions and Electrons." Phys. Rev., Vol. 121, No. 2, 1961, pp. 505-7.

3. Giovanelli, R. G. "Hydrogen Atmospheres in the Absence of Thermodynamic Equilibrium, Parts I, II, III." 1948, pp. 275-318.

4. Fowler, R. H. Statistical Mechanics. Cambridge University Press, London, 1955.

5. Motley, R. W. and Kuckes, A. F. "Recombination in a Helium Plasma." Proceedings of the Fifth International Conference on Ionization Phenomena in Gases, Vol. I., Munich, Germany, 1961. North-Holland Publishing Co., Amsterdam, The Netherlands, 1962, pp. 651-9.

6. Hinnov, E. and Hirschberg, J. G. "Spectroscopic Measurement of Helium Afterglow." Proceedings of the Fifth International Conference on Ionization Phenomena in Gases, Vol. I., Munich, Germany, 1961. North-Holland Publishing Co., Amsterdam, The Netherlands, 1962, pp. 638-50.

7. Bates, D. R., Kingston, A. E., and McWhirter, R. W. P. "Recombination between Electrons and Atomic Ions. I. Optically Thin Plasmas." Proc. Roy. Soc. (London), A267, 1962, pp. 297-312.

8. Bates, D. R., Kingston, A. E., and McWhirter, R. W. P. "Recombination between Electrons and Atomic Ions. II. Optically Thick Plasmas." Proc. Roy. Soc. (London), A270, 1962, pp. 155-167.

9. Gryzinski, M. "Classical Theory of Electronic and Ionic Inelastic Collisions." Phys. Rev., Vol. 115, 1959, pp. 374-83.

10. Hinnov, E. and Hirschberg, J. G. "Electron-Ion Recombination in Dense Plasmas." Phys. Rev., Vol. 125, No. 3, 1962, pp. 795-801.

11. Byron, S., Stabler, P. C., and Bortz, P. I. "Electron-Ion Recombination by Collisional and Radiative Processes." Phys. Rev. Letters, Vol. 8, No. 9, 1962, pp. 376-9.

12. Byron, S., Bortz, P. I., and Russel, G. R. "Electron-Ion Reaction Rate Theory: Determination of the Properties of Non-Equilibrium Monatomic Plasmas in MHD Generators and Accelerators and in Shock Tubes." Proceedings of the Fourth Symposium on the Engineering Aspects of Magnetohydrodynamics, Berkeley, California, April 1963. University of California Press, Berkeley, 1963, pp. 93-101.

13. Petschek, H. and Byron, S. "Approach to Equilibrium Ionization behind Strong Shock Waves in Argon." Ann. Phys., Vol. 1, No. 3., 1957, pp. 270-315.

14. Moore, C. E. "Tables of Atomic Energy Levels." National Bureau of Standards Circular 467, Washington, D. C., 1949.

15. Curry, B. P. "Electron-Collision-Induced Ionization and Recombination in Hydrogenic Plasmas." Bull. Am. Phys. Soc., Vol. 10, No. 2, 1965, p. 263.

16. Fermi, E. Notes on Quantum Mechanics. University of Chicago, Press, Chicago, Ill., 1960.

17. Dugan, J. V., Jr. "Three-Body Collisional Recombination of Cesium Seed Ions and Electrons in High Density Plasmas with Argon Carrier Gas." NASA TN-D-2004, 1964.

18. Robben, F., Kunkel, W. B., and Talbot, L. "Spectroscopic Study of Electron Recombination with Monatomic Ions in a Helium Plasma." Phys. Rev., Vol. 132, No. 6, 1963, pp. 236-71.

19. Wada, J. T. and Knechtli, R. C. "Measurements of Electron-Ion Recombination in a Thermal Cesium Plasma." Phys. Rev. Letters, Vol. 10, No. 12, 1963, pp. 513-16.

20. Harris, L. P. "Ionization and Recombination in Cesium-Seeded Plasmas near Thermal Equilibrium." General Electric Research Laboratory Report 64-RL-31985, Schenectady, New York, 1964.

21. Condon, E. U. and Shortley, G. H. The Theory of Atomic Spectra. Cambridge University Press, London, 1957.

22. White, H. E. Introduction to Atomic Spectra. McGraw-Hill Book Co., New York, 1934.

23. Margenau, H. and Murphy, G. M. Mathematics of Physics and Chemistry, Van Nostrand, New York, 1956.

24. Kech, J. C. and Makin, B. "Variational Theory of Three-Body Electron Ion Recombination Rates." Avco Everett Research Laboratory Report 158, 1963.

25. Seaton M. J. Article in Atomic and Molecular Processes. Edited by D. R Bates, Academic Press, New York, 1962.

26. Omidvar, K. "Theory of the 2S and 2P Excitation of the Hydrogen Atom Induced by Electron Impact." NASA TN-D-2145, 1964.

27. Lichten, W. and Schultz, G. "Cross Sections for the Excitation of the Metastable 2S State of Atomic Hydrogen by Electron Collision." Phys. Rev., Vol. 116, No. 5, 1959, pp. 1132-9.

28. Stebbings, R. F., Fite, W. L., Hummer, D. G., and Brackmann, R. T. "Collisions of Electrons with Hydrogen Atoms. V. Excitation of Metastable 2S Hydrogen Atoms." Phys. Rev., Vol. 119, No. 6, 1960, pp. 1939-45.

29. Kingston, A. E. "Excitation and Ionization of Hydrogen Atoms by Electron Impact." Phys. Rev., Vol. 135, No. 6A, 1964, pp. A1529-A1536.

30. Cool, T. A. and Zukoski, E. E. "Recombination Rates and Non-Equilibrium Electrical Conductivity in Seeded Plasmas." Proceedings of the Sixth Symposium of Engineering Aspects of Magnetohydrodynamics, Pittsburgh, Pennsylvania, April 1965.

31. Kolb, A. C. and Griem, H. R. Article in Atomic and Molecular Processes. Edited by D. R. Bates, Academic Press, New York, 1962.

32. Menzel, D. H. and Pekeris, C. L. "Adsorption Coefficients and H Line Intensities." Monthly Notices, Roy. Astron. Soc., Vol. 96, 1935, pp. 77-111.

33. Stone, P. M. "Cesium Oscillator Strengths." Phys. Rev., Vol. 127, No. 4, 1962, pp. 1151-6.

34. Lutz, M. "Radiant Energy Loss from a Cesium-Argon Plasma to an Infinite Plane Parallel Enclosure." Avco Everett Research Laboratory Report 175, 1963.

35. Zukoski, E. E., Cool, T. A., and Gipson, E. G. "Experiments Concerning Nonequilibrium Conductivity in a Seeded Plasma." AIAA Journal, Vol. 2, No. 8, 1964, pp. 1410-17.

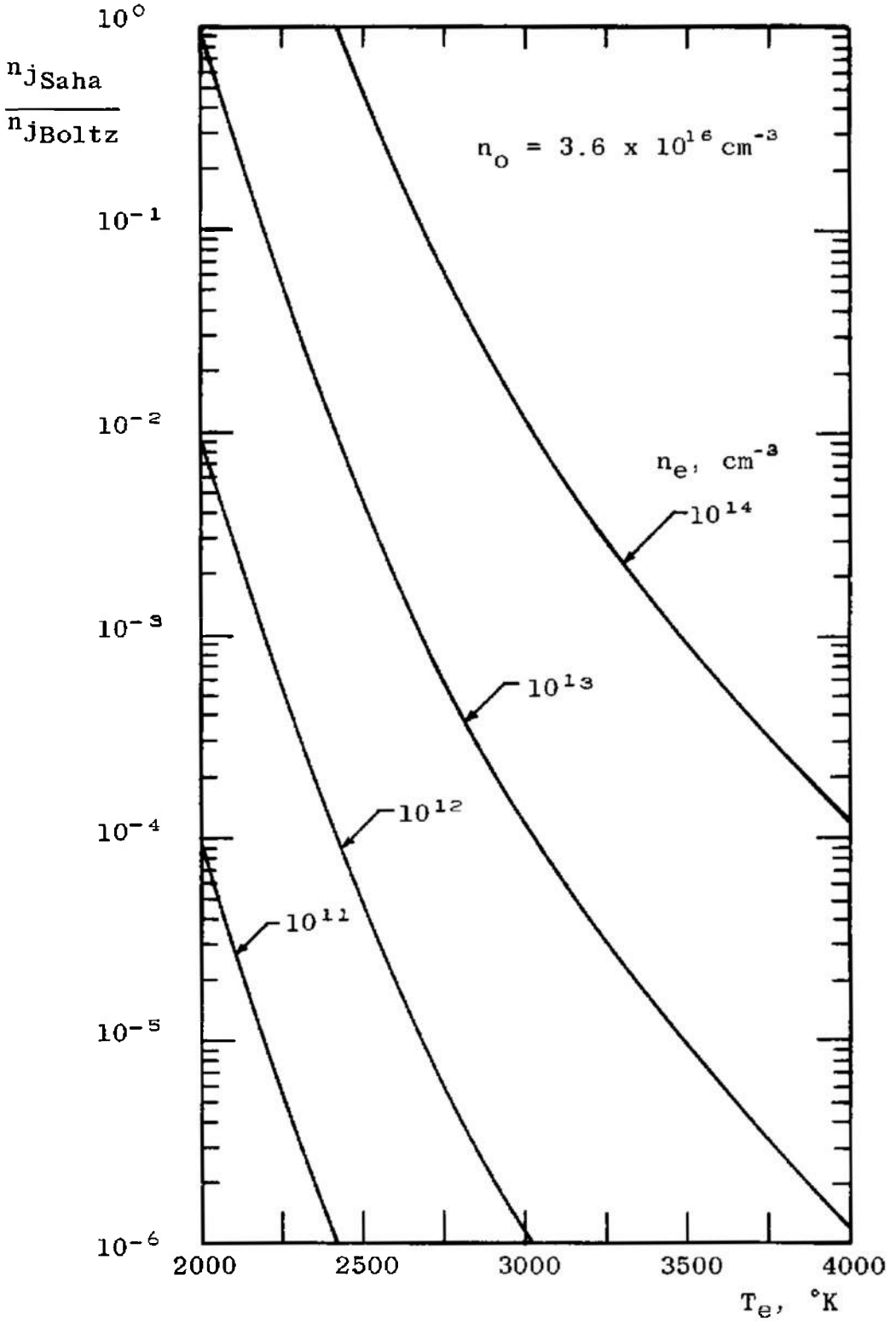

Fig. 1 Ratio of Excited State Populations in Saha Equilibrium with Free Electrons and Boltzmann Equilibrium with Ground State for Potassium

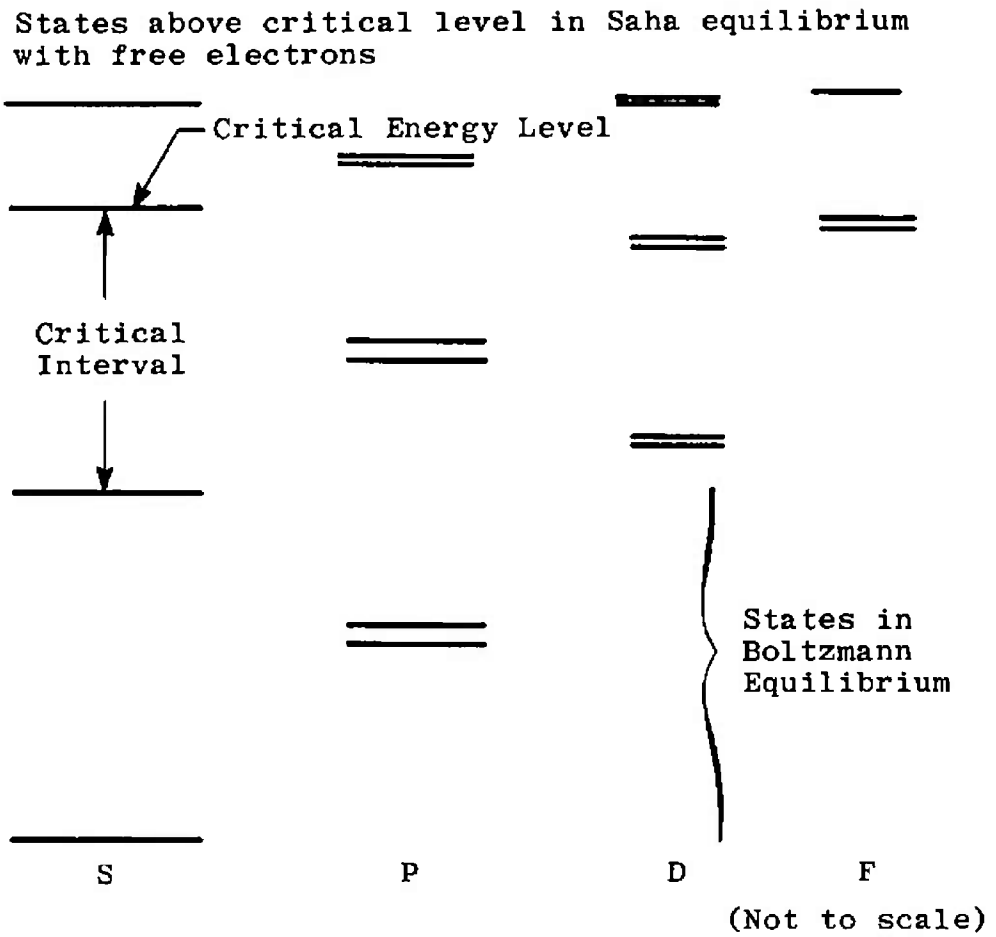

Fig. 2 Alkali Energy Level Diagram Showing Effect of Collisional Transitions

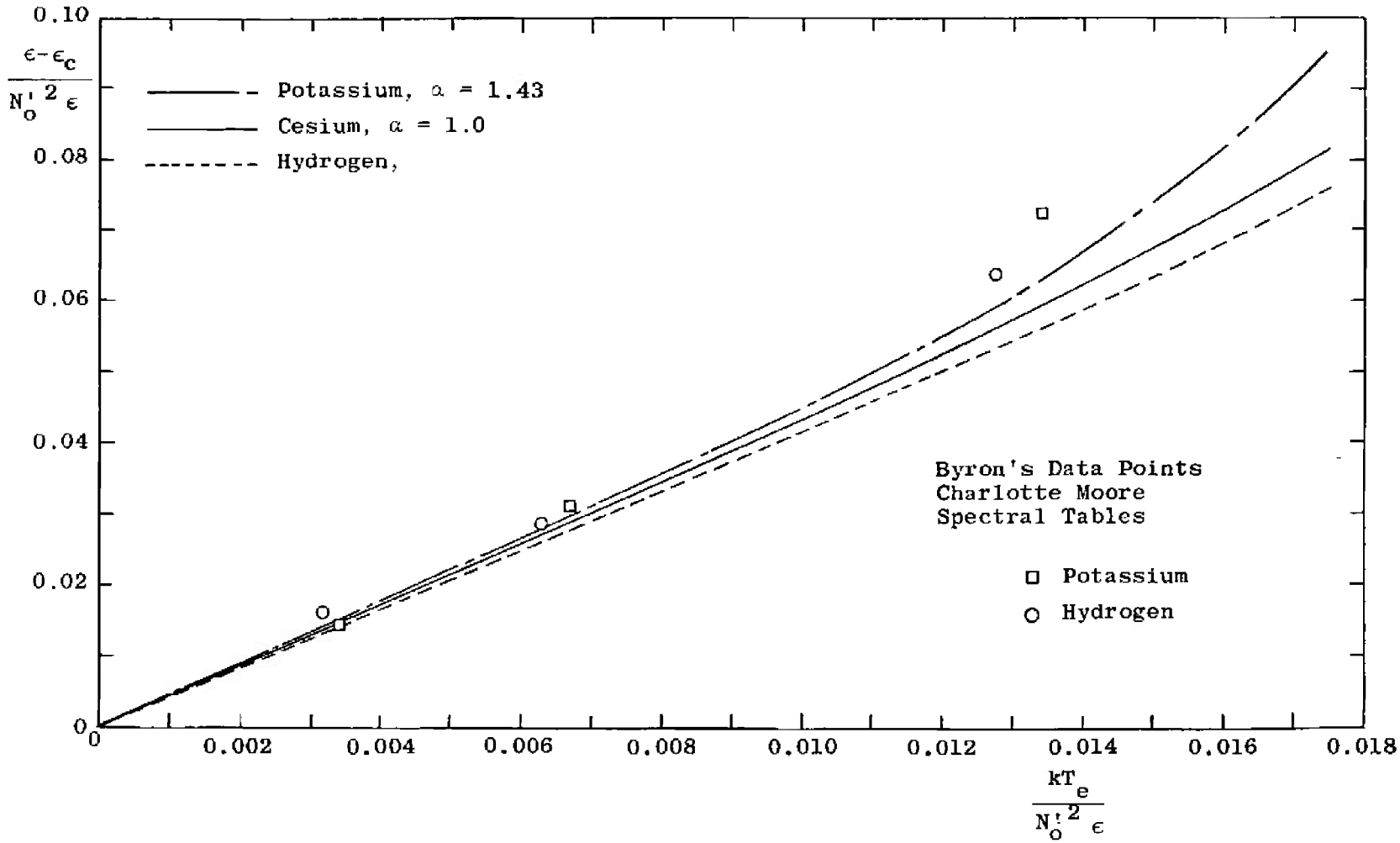

Fig. 3 Critical Energy Level in Equilibrium with Free Electrons

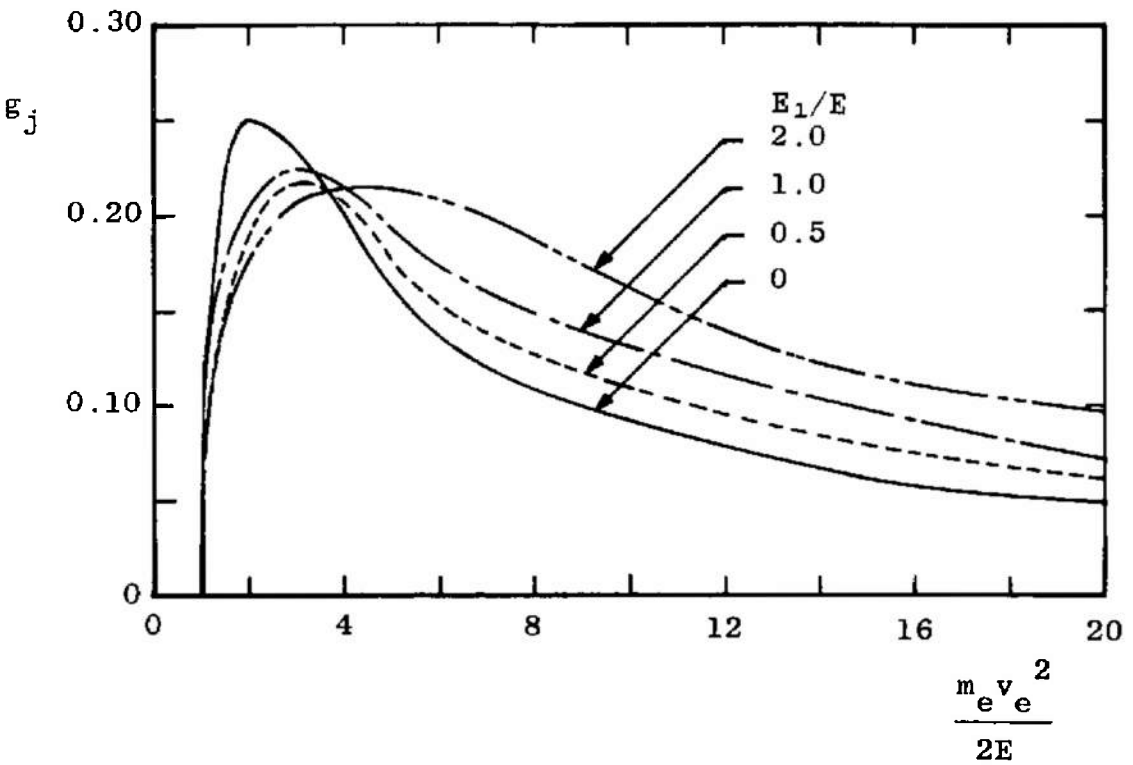

Fig. 4 Gryzinski's Function, g_j (from Ref. 9)

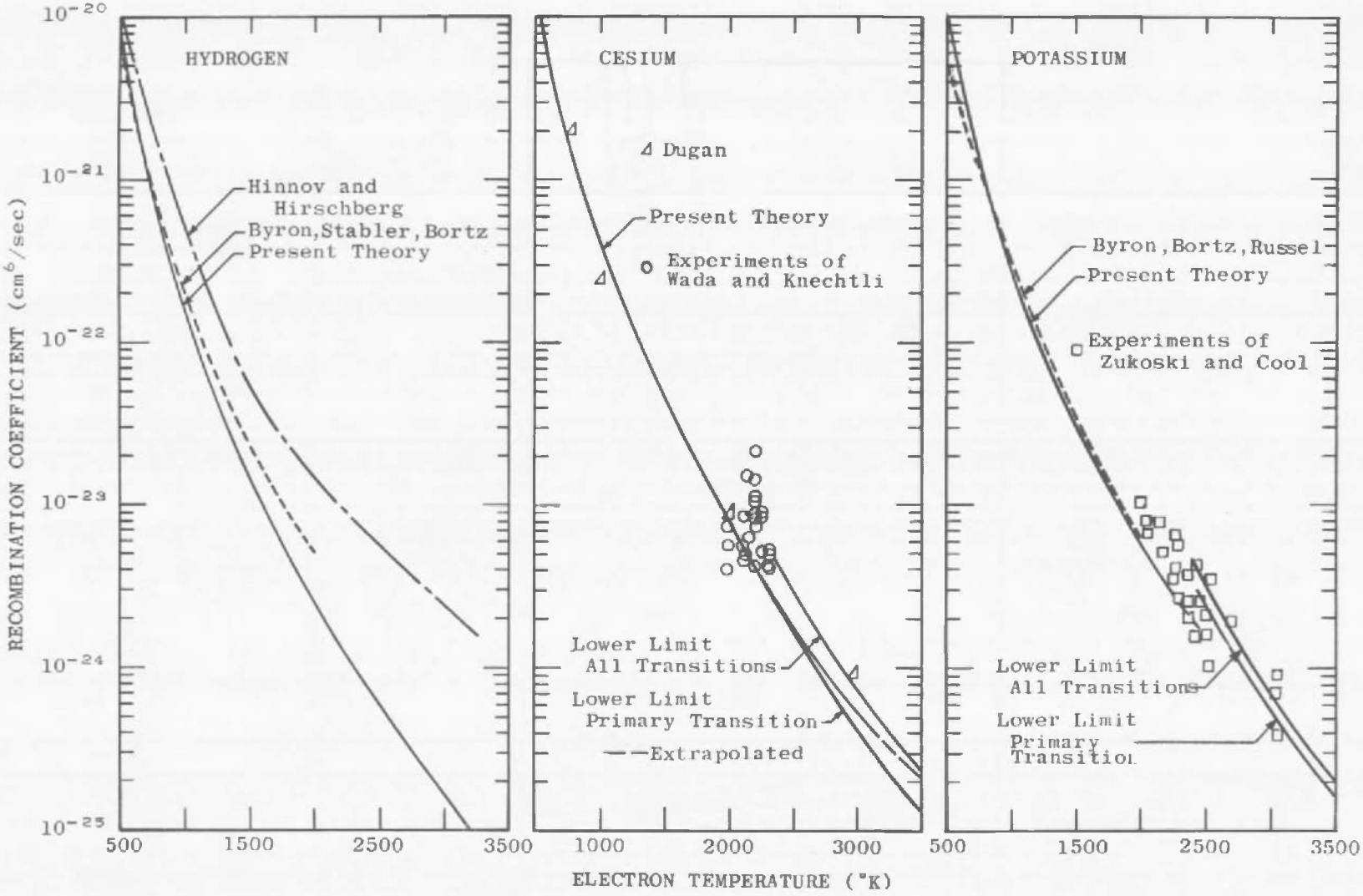

Fig. 5 Collisional Recombination Rates for Hydrogenic Elements

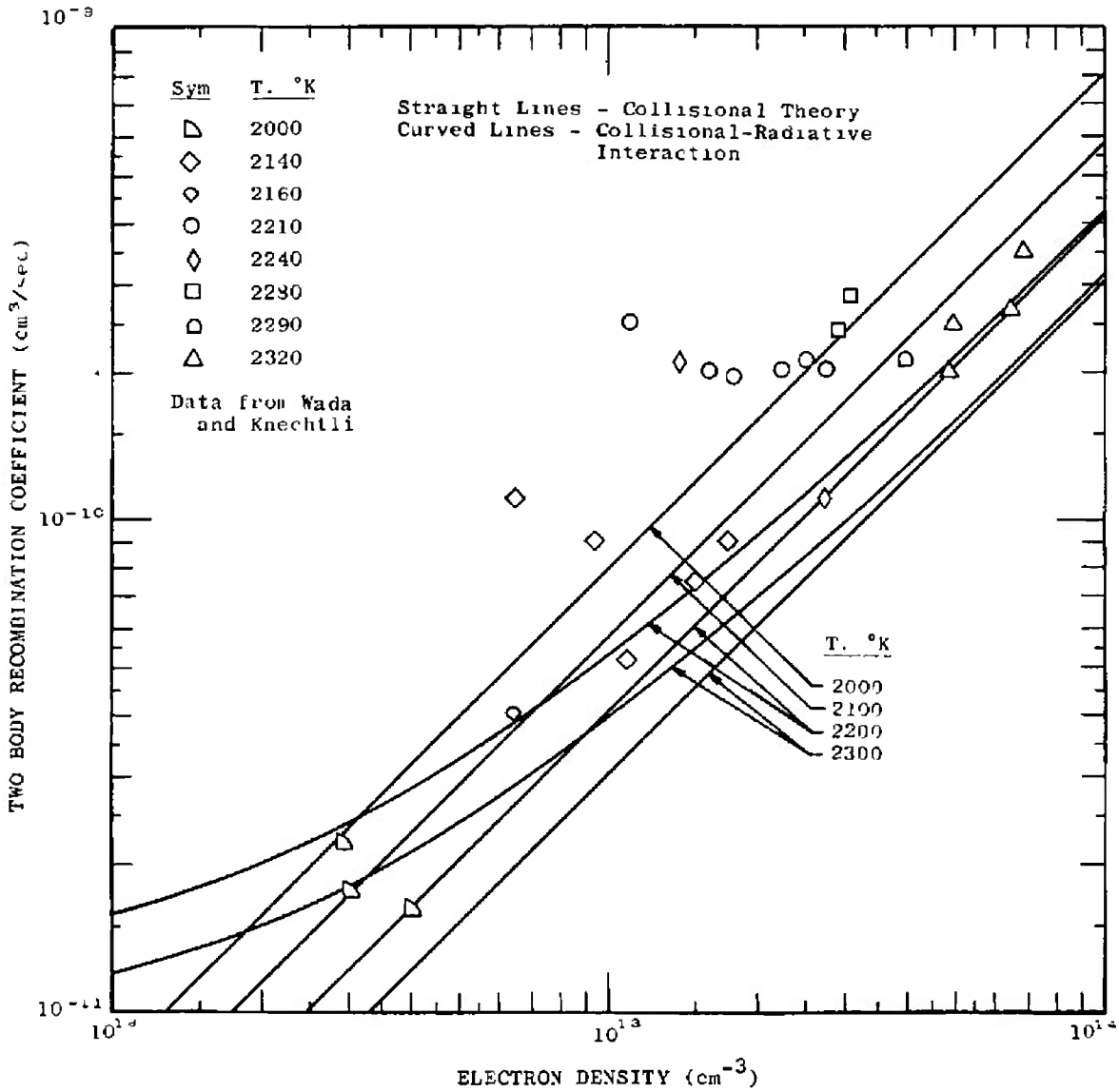

Fig. 6 Electron-Ion Recombination Coefficient as a Function of Electron Density

TABLE I
INTENSITY OF ALLOWED RADIATIVE TRANSITIONS ACROSS VARIOUS CRITICAL INTERVALS

INTERVAL	TRANSITION	OSCILLATOR STRENGTH
7S – 6S	$7S_{1/2} - 6P_{3/2}$	0.21
	$6P_{3/2} - 6S_{1/2}$	0.81
	Composite	0.41
	$7S_{1/2} - 6P_{1/2}$	0.17
	$6P_{1/2} - 6S_{1/2}$	0.39
	Composite	0.26
	$6D_{5/2} - 6P_{3/2}$	0.33
	$6P_{3/2} - 6S_{1/2}$	0.81
	Composite	0.52
	$6D_{3/2} - 6P_{3/2}$	0.04
	$6P_{3/2} - 6S_{1/2}$	0.81
	Composite	0.18
	$6D_{3/2} - 6P_{1/2}$	0.30
	$6P_{1/2} - 6S_{1/2}$	0.39
	Composite	0.34
	$7P_{3/2} - 6S_{1/2}$	0.02
Sum of Oscillator Strengths		1.73
7P – 6P	$7P_{3/2} - 7S_{1/2}$	1+
	$7S_{1/2} - 6P_{3/2}$	0.21
	Composite	0.46
	$7P_{3/2} - 7S_{1/2}$	1+
	$7S_{1/2} - 6P_{1/2}$	0.17
	Composite	0.41
	$7P_{3/2} - 5D_{5/2}$	1-
	$5D_{5/2} - 6P_{3/2}$	0.20
	Composite	0.45
	$7P_{1/2} - 5D_{3/2}$	0.21
	$5P_{3/2} - 6P_{1/2}$	0.25
	Composite	0.23
	$7P_{1/2} - 5D_{3/2}$	0.65
	$5D_{3/2} - 6P_{1/2}$	0.25
	Composite	0.41
	$7P_{3/2} - 6S_{1/2}$	0.02
	$8S_{1/2} - 6P_{3/2}$	0.02
	$8S_{1/2} - 6P_{1/2}$	0.02
Sum of Oscillator Strengths		2.01

TABLE I (Concluded)

6D – 5D	$6D_{5/2} - 7P_{3/2}$	0.31
	$7P_{1/2} - 5D_{5/2}$	1+
	Composite	0.56
	$6D_{3/2} - 7P_{1/2}$	0.33
	$7P_{1/2} - 5D_{3/2}$	0.65
	Composite	0.46
	$8S_{1/2} - 7P_{3/2}$	0.33
	$7P_{3/2} - 5D_{5/2}$	1+
	Composite	0.58
	$8S_{1/2} - 7P_{1/2}$	0.30
	$7P_{3/2} - 5D_{3/2}$	0.69
	Composite	0.44
	$4F - 5D_{3/2}$	0.32
	$4F - 5D_{5/2}$	0.30
	$6D_{3/2} - 6P_{3/2}$	0.33
	$6D_{3/2} - 6P_{1/2}$	0.30
Sum of Oscillator Strengths		3.29
8S – 7S	$8S_{1/2} - 7P_{3/2}$	0.33
	$7P_{3/2} - 7S_{1/2}$	1+
	Composite	0.58
	$8S_{1/2} - 7P_{1/2}$	0.30
	$7P_{1/2} - 7S_{1/2}$	0.56
	Composite	0.41
	$8P_{3/2} - 7S_{1/2}$	0.03
	$4F - 5D_{3/2}$	0.32
	$4F - 5D_{5/2}$	0.30
	$8S_{1/2} - 6P_{3/2}$	0.02
	$8S_{1/2} - 6P_{1/2}$	0.02
Sum of Oscillator Strengths		1.68
8P – 7P	$8P_{3/2} - 7S_{1/2}$	0.03
	$9S_{1/2} - 7P_{3/2}$	0.03
	$9S_{1/2} - 7P_{1/2}$	0.03
	$7D_{5/2} - 7P_{3/2}$	0.28
	$7D_{3/2} - 7P_{1/2}$	0.03
	$7D_{3/2} - 7P_{3/2}$	0.24
	$8P_{3/2} - 5D_{5/2}$	0.22
	$8P_{3/2} - 5D_{3/2}$	0.03
	$8P_{1/2} - 5D_{1/2}$	0.09
	$9P_{3/2} - 5D_{3/2}$	0.07
	$9P_{3/2} - 5D_{5/2}$	0.01
	$9P_{1/2} - 5D_{3/2}$	0.03
Sum of Oscillator Strengths		1.19

TABLE II
EFFECTIVENESS OF LINE RADIATION VERSUS COLLISIONAL TRANSITIONS ACROSS VARIOUS CRITICAL INTERVALS

INTERVAL	SUMMED OSCILLATOR STRENGTHS	$n_e \chi$ (cm^{-3})
7S – 6S	1.73	1.24×10^{14}
7P – 6P	2.01	2.18×10^{13}
6D – 5D	3.29	2.13×10^{13}
8S – 7S	1.68	2.88×10^{12}
8P – 7P	1.19	5.18×10^{11}

Security Classification

DOCUMENT CONTROL DATA - R&D

(Security classification of title, body of abstract and indexing annotation must be entered when the overall report is classified)

1 ORIGINATING ACTIVITY (Corporate author)	2a REPORT SECURITY CLASSIFICATION
Arnold Engineering Development Center ARO, Inc., Operating Contractor Arnold Air Force Station, Tennessee	UNCLASSIFIED
	2b GROUP N/A

3 REPORT TITLE

IONIZATION AND RECOMBINATION IN ALKALI-SEEDED COLLISION-DOMINATED PLASMAS

4 DESCRIPTIVE NOTES (Type of report and inclusive dates)

N/A

5 AUTHOR(S) (Last name, first name, initial)

B. P. Curry, ARO, Inc.

6 REPORT DATE	7a TOTAL NO OF PAGES	7b NO OF REFS
February 1966	49	35

8a CONTRACT OR GRANT NO	9a ORIGINATOR'S REPORT NUMBER(S)
AF40(600)-1200 b Program Element 65402234	AEDC-TR-65-260
c	9b OTHER REPORT NO(S) (Any other numbers that may be assigned this report)
d	N/A

10 AVAILABILITY/LIMITATION NOTICES

Qualified users may obtain copies of this report from DDC. The distribution of this document is unlimited.

11 SUPPLEMENTARY NOTES	12 SPONSORING MILITARY ACTIVITY
N/A	Arnold Engineering Development Center, Air Force Systems Command, Arnold Air Force Station, Tennessee

13 ABSTRACT

At electron densities greater than 10^{-12}/cc, ionization and recombination proceed predominantly by sequential transitions between adjacent energy levels induced by collisions with free electrons. Similar models for this process have been developed by various investigators. This report develops closed-form expressions for ionization and recombination of effective one-electron atoms by modifying the Byron model and determining analytically the critical energy level in equilibrium with the free electrons, using a simplified quantum mechanical model of the alkali atoms. The reaction rate coefficients calculated from these expressions agree satisfactorily with available experimental data and with numerical calculations of other investigators.

DD FORM 1 JAN 64 1473

Security Classification

14 KEY WORDS	LINK A		LINK B		LINK C	
	ROLE	WT	ROLE	WT	ROLE	WT
plasmas						
ionization						
recombination						
alkali-seeded						
collision-dominated						
free electrons						
quantum mechanics						
magnetohydrodynamics						

INSTRUCTIONS

1. ORIGINATING ACTIVITY: Enter the name and address of the contractor, subcontractor, grantee, Department of Defense activity or other organization *(corporate author)* issuing the report.

2a. REPORT SECURITY CLASSIFICATION: Enter the overall security classification of the report. Indicate whether "Restricted Data" is included. Marking is to be in accordance with appropriate security regulations.

2b. GROUP: Automatic downgrading is specified in DoD Directive 5200.10 and Armed Forces Industrial Manual. Enter the group number. Also, when applicable, show that optional markings have been used for Group 3 and Group 4 as authorized

3. REPORT TITLE: Enter the complete report title in all capital letters. Titles in all cases should be unclassified. If a meaningful title cannot be selected without classification, show title classification in all capitals in parenthesis immediately following the title.

4. DESCRIPTIVE NOTES. If appropriate, enter the type of report, e.g., interim, progress, summary, annual, or final. Give the inclusive dates when a specific reporting period is covered.

5. AUTHOR(S) Enter the name(s) of author(s) as shown on or in the report. Enter last name, first name, middle initial. If military, show rank and branch of service. The name of the principal author is an absolute minimum requirement.

6. REPORT DATE: Enter the date of the report as day, month, year, or month, year. If more than one date appears on the report, use date of publication.

7a. TOTAL NUMBER OF PAGES: The total page count should follow normal pagination procedures, i.e., enter the number of pages containing information.

7b. NUMBER OF REFERENCES: Enter the total number of references cited in the report.

8a. CONTRACT OR GRANT NUMBER: If appropriate, enter the applicable number of the contract or grant under which the report was written.

8b, 8c, & 8d. PROJECT NUMBER: Enter the appropriate military department identification, such as project number, subproject number, system numbers, task number, etc.

9a. ORIGINATOR'S REPORT NUMBER(S). Enter the official report number by which the document will be identified and controlled by the originating activity. This number must be unique to this report.

9b. OTHER REPORT NUMBER(S): If the report has been assigned any other report numbers *(either by the originator or by the sponsor)*, also enter this number(s).

10. AVAILABILITY/LIMITATION NOTICES: Enter any limitations on further dissemination of the report, other than those imposed by security classification, using standard statements such as:

(1) "Qualified requesters may obtain copies of this report from DDC."

(2) "Foreign announcement and dissemination of this report by DDC is not authorized."

(3) "U. S. Government agencies may obtain copies of this report directly from DDC. Other qualified DDC users shall request through _____."

(4) "U. S. military agencies may obtain copies of this report directly from DDC. Other qualified users shall request through _____."

(5) "All distribution of this report is controlled. Qualified DDC users shall request through _____."

If the report has been furnished to the Office of Technical Services, Department of Commerce, for sale to the public, indicate this fact and enter the price, if known.

11. SUPPLEMENTARY NOTES: Use for additional explanatory notes.

12. SPONSORING MILITARY ACTIVITY: Enter the name of the departmental project office or laboratory sponsoring *(paying for)* the research and development. Include address.

13 ABSTRACT: Enter an abstract giving a brief and factual summary of the document indicative of the report, even though it may also appear elsewhere in the body of the technical report. If additional space is required, a continuation sheet shall be attached.

It is highly desirable that the abstract of classified reports be unclassified Each paragraph of the abstract shall end with an indication of the military security classification of the information in the paragraph, represented as *(TS), (S), (C), or (U)*

There is no limitation on the length of the abstract. However, the suggested length is from 150 to 225 words.

14. KEY WORDS: Key words are technically meaningful terms or short phrases that characterize a report and may be used as index entries for cataloging the report Key words must be selected so that no security classification is required. Identifiers, such as equipment model designation, trade name, military project code name, geographic location, may be used as key words but will be followed by an indication of technical context The assignment of links, rules, and weights is optional